



# Charming

## Components for Highly Advanced time-Resolved fluorescence Microscopy based on Nonlinear Glass fibres

**FP7 Call identifier:** FP7-ICT-2011-7

**Activity code:** ICT-2011.3.5: Photonics

**Project start date and duration:** 01.09.2011 for 3.5 years

**Contract type:** STREP

**Grant Agreement number:** 288786

### Deliverable 1.11 PROJECT FINAL REPORT

**Period covered:** from 01.09.2011 to 28.02.2015

#### Lead contractor for this deliverable

**Name:** MULTITEL

**Contact Person:** Y. Hernandez

**Address:** 2 Rue Pierre et Marie Curie, 7000, Mons

**Phone:** +32 65 34 28 30

**Fax:** +32 65 34 28 30

**E-mail:** hernandez@multitel.be

#### Supervisor for this deliverable

**Name:** Yves Hernandez

**Contact Person:** Partner or All partners (if PMC)

**Date of approval** (and sharing of the deliverable with PMC) : 27/07/2015

**Authors:** Yves Hernandez, Sebastien, Guillemet, Thomas Schoenau, Alexey Gladyshev, Walter Margulis, Wolfgang Zeller, Laurent Lablonde, Costantino Corbari.

**Participants:** MULTITEL, ACREO, ORC, Nanoplus, IXFIBER, FORC, PicoQuant GmbH

**Workpackage:** WP 1

**Est. person months:**

**Version :** 5 (20/07/2015)

**Security:** PU

**Nature:** Report

**Total number of pages :** 51



*Any work or result described in this report is in principle genuinely a result of this project. When some results from other work or projects are used, related sources are properly referenced in the text.*



## History :

Version	Date	Modifications/comments	Author
1	01.04.2015	Initial document	Y. Hernandez
2	07.04.2015	Inputs from partners	T. Schoenau, A. Gladyshev, L. Lablonde.
3	11.04.2015	Finalisation of the document with last inputs.	W. Margulis, W. Zeller.
4	04.06.2015	Modifications after review	All partners
5	20.07.2015	Addition of dissemination tables and list of patents	Y. Hernandez

## Validation :

Author	Date	Signature
Y. Hernandez	20/07/2015	
Reviewer	Date	Signature
PMC	27/07/2015	



## Table of content

1. Final publishable summary .....	5
1.1. Charming project in brief .....	5
1.2. Executive summary .....	6
1.3. Summary description of project context and objectives .....	7
1.4. Description of the main S&T results/foregrounds .....	9
1.4.1. WP3: Optical fibres development .....	9
1.4.1.1. Bismuth doped fibres .....	9
1.4.1.2. Micro-structured fibres .....	10
1.4.1.3. Poling of twin hole and micro-structured fibres .....	11
1.4.2. WP4: Non linear devices development .....	12
1.4.2.1. Improvements in fabrication: low temperature electrodes filling and removal ...	12
1.4.2.2. Long devices periodic erasure and validation of new wavelength for erasure .....	13
1.4.2.3. Realization of different devices with high performances demonstration .....	16
a) Watt level SHG in fibres at 772 nm .....	16
b) 521 nm in-fibre, frequency conversion with a gain-switched laser .....	17
c) 560 nm in-fibre, frequency conversion with a mode-lock laser .....	19
d) 560 nm in-fibre, frequency conversion with a gain-switched laser .....	20
e) 590 nm in-fibre, frequency conversion with a gain-switched laser .....	21
f) Increase of efficiency: concatenation of devices .....	23
1.4.2.4. Single pulse selection .....	23
1.4.2.5. Packaging .....	24
1.4.3. WP5: Narrow linewidth pulsed laser sources .....	25
1.4.3.1. New high power diodes at 1180 nm for gain-switching .....	25
1.4.3.2. New gain-switched devices at 1180 nm. ....	26
1.4.3.3. Raman amplification at 1180 nm. ....	27
1.4.4. WP6: Devices and lasers integration .....	29
1.4.4.1. Confocal and STED experiments .....	29
1.4.5. WP7: Demonstration .....	29
1.4.5.1. Fibre devices integration with gain switched lasers .....	29
1.4.5.2. Demonstration of 559 nm pulsed source for FLIM applications .....	30
1.4.5.3. Demonstration of 266 nm pulsed source for tryptophan spectroscopy .....	31
1.4.5.4. Demonstration of 355 nm pulsed source for fluorescence spectroscopy .....	32
1.5. General conclusion and potential exploitable results .....	33
1.6. Potential impact .....	33
1.6.1. Potential markets: .....	34
1.6.1.1. Biomedical applications .....	34
1.6.1.2. DFB diodes .....	35
1.6.1.3. Athermal packaging for long fibre devices .....	36
1.6.1.4. Periodically poled fibre devices .....	36
1.6.1.5. Electro-optic fibre devices .....	36
1.6.2. Social impact: .....	36
1.6.3. Dissemination and exploitation tables .....	38
1.6.3.1. List of scientific publications .....	38
1.6.3.2. List of dissemination activities .....	41



---

1.6.3.3. List of patents and trademarks.....	45
2. Report on societal implications.....	46

## 1. Final publishable summary

### 1.1. Charming project in brief

Charming means “Components for Highly Advanced time-Resolved fluorescence Microscopy based on Nonlinear Glass fibres”. The aim of this project was then to develop new diagnosis tools providing high resolution in compact and rapid systems.

Super-resolution techniques like STED and photo-switching microscopy are just opening the doors to a truly new dimension in optical microscopy for bio-imaging. For the first time it is not only possible to really “see” the structure of cell organelles in much more detail but also to study for example the internal structure of bacteria, with a size typically far below the optical diffraction limit.

Fluorescence Lifetime Imaging Systems (FLIM) are applied in many biomedical fields. This technique can for instance, be applied in in vivo studies to localize tumors and detect their progression with adapted fluorophores.

The most promising direction in this field is for safe in-vivo skin and tissue characterisation to identify tumours and other specific defects based on a lifetime assisted auto-fluorescence imaging. In recent years, several research consortia started to develop instruments for medical diagnosis for epidermal skin imaging, ophthalmology and endoscopic imaging inside living specimen.

CHARMING contributed to this field of activity by providing new laser sources which are essential for the development of all these diagnostic tools that are more and more routinely used for screening pathologies at early stage.

## 1.2. Executive summary

The project CHARMING aimed at developing compact and fully fibred visible lasers for fluorescence spectroscopy and high resolution confocal microscopy systems. Various visible lasers are required for these applications, with the following characteristics:

- \* Picosecond pulses at repetition rates adjustable from 1 MHz to 80 MHz;
- \* Average output power from 5 mW to 500 mW (at 40 MHz or 80 MHz);
- \* Polarization maintaining single-mode output, with very stable pointing.

As a result the project achieved various impressive results in terms of new laser sources, fundamental understanding of the physics of these non linear devices and state of the art performances like for instance:

- demonstration of high power SHG generation in fibre (>2W at 775 nm),
- all-fibre pulse picking at MHz regime,
- gain-switched sources at 1120 and 1180 nm,
- picoseconds pulses amplification at 1120 and 1180 nm,
- various all-fibre visible sources in pulsed regime, based on gain-switched and mode-locked lasers (521 nm, 560 nm, 590 nm).

From this project various results will be commercially exploited like:

- New designs for high power DFB semiconductor diodes for gain-switching,
- New PM coupled butterfly DFB sources for gain-switching at 1120 and 1180 nm.
- New gain-switched modules at 1120 and 1180 nm,
- High power amplifiers at 1120 and 1180 nm,
- Picosecond sources at 590/295 nm as a future product.
- Picosecond laser sources with high maturity level at different wavelengths on the visible (766, 355, 266, 561 nm) for fluorescence applications.
- Active and passive packaging units for long fibre devices that can be applied in telecom applications for long dispersion compensation filters for instance.

The project CHARMING has also generated many scientific results that will impact the research in the domain of optical fibres poling in particular:

- Investigation and deep understanding of poling mechanisms in optical fibres,
- Development of a poling method with soft electrodes that can be injected and removed after poling from the optical fibre without degradation of the induced non linearities in the fibre.
- Validation of a new UV inscription wavelength for the periodic erasure of the poling along the optical fibre.
- Development of a complete periodic erasure set-up, permitting the precise and reproducible inscription of long devices in optical fibres.
- Complete understanding of the mechanisms of poling erasure by multi-photons absorption during laser operation.
- Development of a high speed and high extinction ratio electro-optical in-fibre device.

The results of this project will have short term and long term impacts in different application fields like:

- Life science: new diagnostic tools in medicine
- Telecommunications: quantum cryptography for future highly secured data transfer
- Lasers: Ultrashort sources for various domains like micromachining for instance.
- Sensors: High Voltage sensing

More information can be found in the CHARMING website (<http://www.charming-project.eu/>) or through the youtube project videos (<http://www.charming-project.eu/videos.html>) explaining all the steps from the optical fibres and semiconductors design to the biomedical imaging application.

### 1.3. Summary description of project context and objectives

Today semiconductor laser diodes are available from 350 to 500 nm. To cover the spectra between 515 nm and 630 nm frequency conversion technologies are employed. In order to guarantee a perfect Gaussian beam overlap between all wavelengths, free space frequency doubling and subsequent fibre coupling is used. This solution suffers from important drawbacks in terms of stability, compactness and cost.

Additionally given the emission band possibilities of currently used species in solid-state lasers and amplifiers like Neodym, Ytterbium and Erbium some wavelengths are difficult to reach even though frequency doubling. For instance 560 nm is a very interesting wavelength for fluorescence imaging as it corresponds to classical fluorophors but requires a laser source at 1120 nm. This is at the edge of Ytterbium emission band. As a consequence, this wavelength can be achieved with a specific Ytterbium doped fibre composition, the performances are degraded compared to classical 1064 or 1030 nm bands and fibre and amplifier designs require much more attention. If one considers now 590 nm that can have various applications, not limited to biomedical imaging, the challenge is even higher. Indeed, in order to reach 590 nm through second harmonic generation one needs to develop a fundamental laser source at 1180 nm which is out of reach of Neodym, Ytterbium or Erbium emission bands. The primary semiconductor sources at these wavelengths (1120 and 1180 nm) are also not necessarily available with the required performances (polarization maintaining fibre output, narrow spectrum, good behaviour in pulsed mode). Finally we can add that 590 nm is in particular interesting for depletion in super-resolution microscopy, and to generate 295 nm radiation for Tryptophan imaging. This means that for both applications, in case the challenge was not high enough, a high average power (hundreds of milliwatts in tens of picoseconds regimes) is needed for the 590 nm radiation.

Two main options can be envisaged for tackling this difficulty. The first type of options is to consider amplification at 1180 nm through special fibres like Bismuth doped fibres or Raman gain fibres. The second type of options is to consider direct generation of 590 nm or 295 nm through non linear conversion schemes in crystals like Sum Frequency Generation but this is usual complicated and low efficient.

Then in the project CHARMING we decided to develop these different exotic laser sources using fibre based solutions for the amplification. We tested both Bismuth and Raman amplification for 1180 nm and used Ytterbium for 1120 nm. Regarding the frequency doubling step we also developed in the frame of the project fully fibre based solutions to avoid any free-space alignment in the process. This was of course another important part, the main one, of the challenge of the project CHARMING.

In fact the situation is completely different for these two aspects of the project. Regarding the laser sources, a solution needed to be found where almost no suitable and competitive approach exists. For SHG, the aim was to develop a new approach for a problem that could already be addressed by non ideal but mature and competitive solutions in the market. Indeed SHG can already be addressed by crystal based conversion and use of free space optics to obtain a fibre coupled visible laser source. This results on a less practical solution since the light has to be coupled out of fibre before being converted and reinjected in another fibre with important losses, needs careful and precise alignment steps and is sensitive to external sources of perturbation like vibrations or temperature. Nevertheless SHG in crystals is a very mature technique that permits to achieve high conversion efficiencies allowing to compensate for the light coupling losses in this approach.

Then the situation regarding second harmonic generation in optical fibres was much less mature than crystal based solutions but it does not mean that the objectives were completely out of reach at the project beginning based on the pre-existing knowledge in the consortium. For instance 236 mW had already been generated at 775 nm in fully fibre configuration with a narrow linewidth semiconductor laser source, externally modulated and amplified. This was a record established by partners of the project before the start of CHARMING that has been far outreached within the project.

In this context the project objectives were clear and challenging: develop new visible laser sources in tens of picoseconds regime for different time-resolved fluorescence imaging applications and develop fibre based frequency conversion solutions to permit a higher degree of integration of these fibre laser sources in confocal imaging systems.

Regarding the wavelengths of interest, these are summarized in the following table.

*Table 1: Lasers specifications for Time resolved fluorescence imaging:*



Application		Wavelength	av. Power	prf	Pulse width	beam
Tryptophane fluorescence		295 nm	1 mW	10..20 MHz	100 ps	Collimated
Time-resolved Fluorescence Microscopy		560 nm 590 nm	1..10 mW	10..80 MHz	100 ps	Single mode PM fibre
STED	Excitation	440 nm 510 nm 640 nm	1..10 mW	10..80MHz	100 ps	Single mode PM fibre
	Depletion	590 nm 770 nm	200..500 mW	Sync. to excitation	200..500 ps	Single mode PM fibre
gSTED	Excitation	440 nm 510 nm 640 nm	1..10 mW	160 MHz	100 ps	Single mode PM fibre
	Depletion	cw at gSTED, not part of the project				

From this table our main targets were 295 nm/ 1 mW, 560 and 590 nm / 10 mW, 590 and 770 nm / 200 mW. Other wavelengths like 355 and 266 nm were added by PICOQUANT during the project based on their prospection and continuous update of the market expectations.

These main objectives implied a serie of different intermediate steps and targets to be fulfilled all along the project:

- As the preferred approach for reaching the visible domain was to use second harmonic generation, a first mandatory step was to develop the laser sources at corresponding fundamental wavelengths, i.e. 1120 and 1180 nm in particular. Two options were envisaged for that:
  - o The first and preferred option was direct modulation of semiconductor diodes and subsequent amplification. This is the usual approach employed by PICOQUANT and then the most suitable and compatible solution with their system.
  - o A backup solution envisaged in the project was to use mode-locking at a fundamental repetition rate of 80 MHz combined with in-fibre pulse picking to decrease the frequency of the laser source.
- Whatever the solution for the laser source subsequent amplification steps were required to achieve a suitable optical power for the application. In particular for depletion applications at 1180 nm, one order of magnitude higher power is needed compared to excitation at 1120 nm.
  - o At 1120 nm, Ytterbium amplification was used with the aim to reach the hundreds of milliwatts regime.
  - o At 1180 nm, both Bismuth and Raman amplification were envisaged with the aim to reach the Watt level.
- For frequency doubling both crystal and fibre solutions have been considered in function of the different targets. Of course the main goal is to cover as much as possible applications with the all-fibre configurations:
  - o For conversion down to UV, crystals are the only suitable solutions.
  - o For low power excitation applications, the aim of the project was to demonstrate the possibility to have an all in-fibre wavelength conversion.
  - o For high power depletion applications, fibre based solutions are also experimented, in particular for 775 nm with the aim to demonstrate 50% conversion efficiency for 1 kW peak power signals.
  - o An adapted solution for thermal stabilization of the fibre laser sources is also required for the devices integration. Ideally a passive solution would be preferred but both active and passive solutions are envisaged.

Finally all these developments have to be integrated into demonstrators compatible with FLIM or STED measurements.



## 1.4. Description of the main S&T results/foregrounds

### 1.4.1. WP3: Optical fibres development

#### 1.4.1.1. Bismuth doped fibres

The project CHARMING considered bismuth doped fibres as a possible solution for optical generation and amplification of short pulses (~100 ps) at the wavelength around 1180 nm. The best glass composition for the Bi-doped fibre core with luminescence properties in this region is aluminosilicate fibre (ASB). So far, the most efficient Bi lasers were based on aluminosilicate fibres with low Bi doping and low gain (specific gain  $g_0 < 0.02$  dB/m, the total length of the fibre ~100 m). Such a length is hardly compatible with short pulse generation and amplification.

In “Charming” we try to reach higher  $g_0$  using higher Bi doping levels. **We achieved the net gain as high as  $g_0 = 0.35$  dB/m**, however, the increase of Bi doping level was accompanied by the rise of non-bleachable optical losses, that limits the fibre performance for laser applications. Two fibres (Bi-143 and U15start) were used for laser experiments with the goal to check the efficiency of the lasers based on these fibres. The maximal efficiency of ~3.8% was achieved (U15start). This value is essentially lower in comparison with the efficiency of 20% achieved with the best low Bi concentration and reported in [Dianov et al., J. Opt. Soc. Am. B 24, 1749 (2007)].

To solve the problem of non-bleachable optical losses in fibres with high Bi concentration we optimized the core composition and fibre manufacturing technology on the basis of the following ideas. Bi atoms can exist in silica glass in various valence states. It can be, e.g.,  $\text{Bi}^{3+}$ ,  $\text{Bi}^{2+}$ , ...,  $\text{Bi}^0$ . (Here numbers show not the ion charge but the valence of the atom). Some experiments point to Bi in low valence state as a component of the IR Bi active centre in a silica-based glass. Other experiments enable one to suppose that high level of optical losses in Bi-doped fibres with high Bi content can be due to presence of neutral Bi atoms. So, for better Bi active fibres, it is necessary to reduce  $\text{Bi}^{3+}$  to  $\text{Bi}^{2+}$  (or to  $\text{Bi}^+$ ), but to oxidize  $\text{Bi}^0$  also to low valence Bi ( $\text{Bi}^+$  and  $\text{Bi}^{2+}$ ). To control redox processes, it was proposed to co-dope core glass with cerium (well-known oxidizing agent). The main progress achieved can be summarized with the two following points:

1. The presence of Ce enabled to eliminate the over-reduction of Bi ions in a glass with formation of  $\text{Bi}^0$  clusters and inevitable increase of optical losses. At the same time, it was found that there is a direct relationship between bismuth active centre concentration and induced loss level at room temperature during the pumping process. And for this reason **the effective Bismuth optical amplifiers at the wavelength ~1180 nm can be developed only at low Bismuth active centre concentration corresponding ~1 dB/m absorption at 1.06  $\mu\text{m}$** . At least 2 fibres with better lasing parameters in comparison with all fibres investigated before (with the pump absorption at the level ~1 dB/m) were obtained:
  - Optical gain up to 0.22 dB/m,
  - Bi laser output power 1.3W at the wavelength of 1180 nm
  - Efficiency of 9.5%,
  - Fibber length 45 m,
  - Pump absorption ~1dB/m
  - Room temperature operation.
2. It was confirmed that all Bi-doped aluminosilicate fibres demonstrate essentially better optical gain and reduction of optical losses at lower temperatures: the same Bi laser revealed output power 2.3W (eff. 16.7%, fibre length 45 m) at the temperature of -20°C at the same pump conditions. As a last resort, such a temperature can be maintained in a small part of the device (containing fibre) using thermoelectric elements.

Finally, according to the results obtained so far on Bismuth fibres, it was decided to stop the activity on Bismuth and concentrate on Raman amplification only. Despite of the progress made, the performance of Bi-doped fibres is still not sufficient to integrate them into a commercial product in the frame of CHARMING project.

#### 1.4.1.2. Micro-structured fibres

Micro-structured fibres (MOF) can be used to optimize dispersive properties of the waveguide. In the context of poled fibres for frequency doubling we were interested in determining a fibre geometry ensuring high conversion efficiency over a broad acceptance bandwidth of the periodically poled fibre devices. We also took into account the need for 1) compact size of microstructure, 2) low sensitivity to fibre fabrication tolerances and 3) large QPM-period for periodical poling.

In the frame of CHARMING different MOF designs were developed and analyzed:

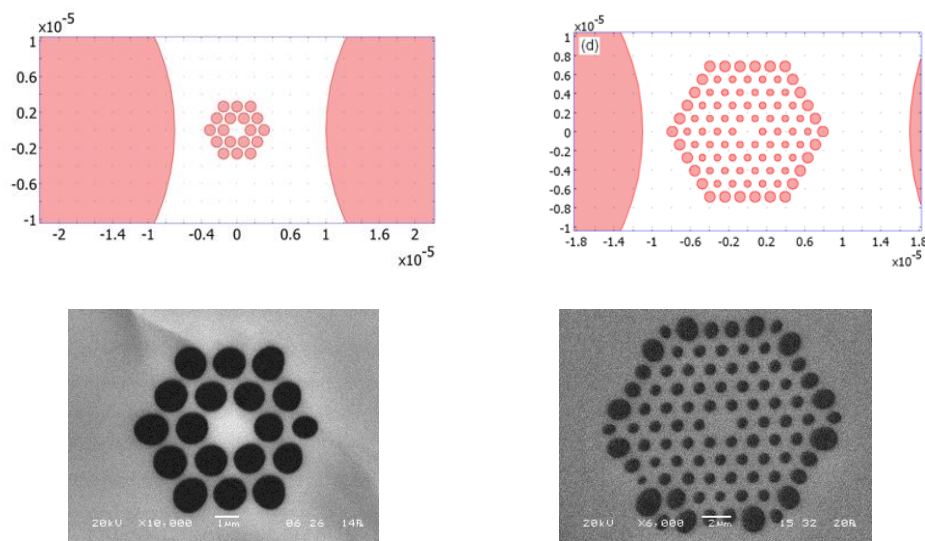


Figure 1: MOF designs for wavelength of 1064 nm (top-left) and 1550 nm (top-right) and corresponding SEM images of the MOFs fabricated for pump wavelength of 1064 nm (bottom-left) and 1550 nm (bottom-right).

Table 2: Geometry of the MOF designs chosen for fabrication:

$\lambda$ ( $\mu\text{m}$ )	rings	$\Lambda$ ( $\mu\text{m}$ )	$d/\Lambda$	$D_s/\Lambda$	$d_{\text{core}}=2*\Lambda-d$ ( $\mu\text{m}$ )
1.064	2	1.52	0.802		1.82
1.55	5	1.58	0.44	0.7	2.06

Table 3: Waveguide properties of the MOF designs chosen for fabrication:

$\lambda$ ( $\mu\text{m}$ )	$A_{\text{ovl}}$ ( $\mu\text{m}^2$ )	$\Lambda_{\text{QPM}}$ ( $\mu\text{m}$ )	BW ( $L_f=10$ cm) (nm)	FOM ( $BW^2/A_{\text{ovl}}$ ) $\times 10^{-6}$
1.06	0.56	12.33	8.83 (tol=7% $\Rightarrow$ 1 nm)	139
1.55	6.57	21	205	6396

The MOF design for wavelength of 1064 nm is simple and compact. It is characterized by a grating period 12.3  $\mu\text{m}$ , which is twice as large as in other designs for this wavelength. Bandwidth 8.83 nm and figure of merit (FOM)  $139 \times 10^{-6}$  significantly exceed the values for step-index fibres. Compared to other designs, this design was found to be much less sensitive to fabrication tolerances, in particular to variation of fibre diameter. The bandwidth decreases to the value of 1 nm at  $\sim 7\%$  deviation of the pitch and hole diameter from the optimal value. The core diameter is 1.8-1.9  $\mu\text{m}$  and cannot be increased without loss of bandwidth.

The MOF design for wavelength of 1550 nm has very broad bandwidth of 205 nm and quite long QPM period of 21  $\mu\text{m}$ . However, 5-ring microstructure could potentially be a problem for efficient poling of such a fibre.

New designs with reduced number of rings in the microstructure have been developed for pump wavelength of 1550 nm. An optimized MOF design was chosen for fabrication. The design has enlarged mode field diameter (MFD) and QPM grating period in comparison with the previous design of 5-ring structure (**Erreur ! Source du renvoi introuvable.**). Enlarged MFD improves situation with input coupling and grating formation. The large bandwidth, stable against variation of fibre diameter, remains the main advantage of the chosen designs as compared to conventional fibres.

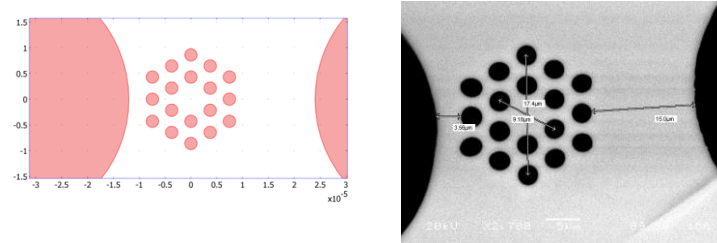


Figure 2: Optimized MOF design for wavelength of 1550 nm (left). Pitch is  $\Lambda = 4.3 \mu\text{m}$  and relative hole size is  $d/\Lambda = 0.56$  and corresponding SEM image of the MOFs fabricated (right).

Table 4: Waveguide properties of the optimized MOF design for  $\lambda=1550 \text{ nm}$  chosen for fabrication:

MFD @1.55 $\mu\text{m}$ ( $\mu\text{m}$ )	NA @1.55 $\mu\text{m}$	$A_{\text{ovl}}$ ( $\mu\text{m}^2$ )	Loss (FM), (dB/m)	$L_{\text{QPM}}$ , ( $\mu\text{m}$ )	BW ( $L_f=10$ cm) (nm)	FOM ( $BW^2/A_{\text{ovl}}$ ) $\times 10^{-6}$
5.19	0.187	19.25	0.32	47.17	20 (29 at 3% scaling)	20.8

A number of technological procedures have been developed at FORC for twin-hole MOF manufacture. Several 15 – 50 m long pieces of twin-hole MOFs have been successfully manufactured according to each of the designs mentioned above.

#### 1.4.1.3. Poling of twin hole and micro-structured fibres

A number of twin-hole and micro-structured fibres for poling were designed, manufactured and characterized during CHARMING. The use of fused silica in the cladding was found to be an efficient way to spread mobile cations with sufficient concentration into the central region of the fibre. Two poling configurations were used, one a conventional arrangement with an anode and a cathode, and the other configuration making use of two internal anodes biased to the positive high voltage (without a connected cathode).

**It was found possible to create a second-order nonlinearity by poling a micro-structured fibre with a pure silica core defined by the surrounding holes.** Different optimized designs were implemented, but the nonlinear coefficient induced was too low to lead to advantageous use in frequency doubling, in spite of the predictions of broader bandwidth for second-harmonic generation.

Twin-hole fibres had cross-section optimized according to the poling configuration to be used. For frequency doubling, most fibres were made with a relatively large hole size that allowed for the insertion of a fine metal wire that could be easily removed after poling. For the electro-optical effect, where internal electrodes are needed for controlling the refractive index after poling, alloy electrodes were employed.

**When we started the project, the nonlinear coefficient was in the range of 0.05-0.15 pm/V. At the project end, we reached values of 0.2-0.45 pm/V.** This was accomplished by realizing the importance of increasing the bias voltage during poling, which led to new fibre designs with appropriate dimensions and in particular holes further from each other. At the end of CHARMING the poling voltage was typically in the neighbourhood of 10 kV.

The increase in second-order nonlinear coefficient led to record-breaking results in terms of conversion efficiency of frequency doubling fibres and performance of single-pulse selectors. In the former, more than 2 W average power red light were generated by a doubling fibre at 775 nm, and in the latter, single-pulse selection from 100 MHz pulse trains with >30 dB extinction ratio were demonstrated. The performance parameters of such devices are described later.

#### **1.4.2. WP4: Non linear devices development**

##### **1.4.2.1. Improvements in fabrication: low temperature electrodes filling and removal**

One significant development of CHARMING is the use of the eutectic alloy BiSn as internal electrode material for poling. When we started our project, we had already tested BiSn for its outstanding advantages, such as low viscosity, no glass wetability, small expansion after solidification, being environmentally friendly and low cost. However, we failed in recording a second-order nonlinearity. We attributed this to the fact that the electrodes are liquid when poling the fibre at 265 °C, since the fusion temperature is 137 °C. We speculated that the liquid metal injected so many new ions into the glass that it was not possible to create a depletion region and record a field. During CHARMING we attempted poling again, this time pressurizing the electrode while poling. At present we use a conventional bicycle pump to this end. The high pressure prevents the liquid from spreading in the hole and breaking into small metal beads. It was found that with the continuous electrode we could induce a slightly larger nonlinear coefficient than with solid electrodes, such as AuSn that melts at 280 °C and is solid during poling. The highest nonlinear coefficients achieved in our project (~0.45 pm/V) had this alloy as electrode.

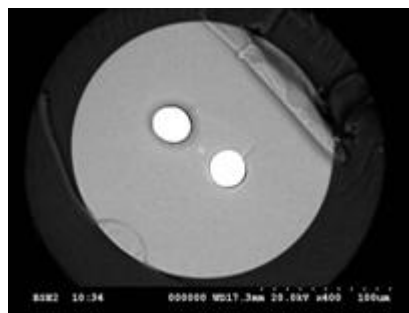


*Figure 3: A fibre for poling with the two-holes filled with BiSn. The cleave is imperfect because the fibre still has the primary coating on (not the case when using the fibre for poling)*

The low melting temperature means that when we start the poling procedure, the fibre provided with electrodes is still completely transparent, since the coating is temperature resistant to 150 °C for hours. One can then easily contact the fibre and inspect for eventual interruptions in the electrodes, which hardly ever happens in components less than 50 cm, but can happen when lengths approach 70-100 cm.

One additional important advantage of BiSn as electrode material is the fact that it expands by 0.5% upon solidification. This causes the fibre to stress in the direction of the hole centres, and causes the fibre to gain a significant birefringence that makes it become polarization maintaining. For long electro-optical devices, this helps meeting the requirements of PM operation even when the fibre is curled into its small footprint package. For frequency doubling, the low melting temperature makes it possible to remove the nearest electrode after poling without erasing the nonlinearity induced. Besides, by keeping the furthest hole to the core filled with the metal, makes

the fibre maintain the polarization, which is necessary when frequency doubling: the conversion efficiency is 9 times higher when the polarization of the IR beam is aligned with the direction of the holes, than when it is orthogonal to it.

The fibres delivered by Acreo to the ORC for periodic erasure and subsequent integration by MULTITEL into a frequency-doubling laser system were poled with BiSn electrodes.

#### 1.4.2.2. Long devices periodic erasure and validation of new wavelength for erasure

The fabrication of efficient periodically poled silica fibres strongly relies on the quality of the  $\chi(2)$ -grating. In CHARMING we have pioneered the use of multi-photon ionization by picosecond pulses at  $\lambda = 355$  nm as a mean to write the quasi-phase matching (QPM) grating. The advantages over the use of UV erasure by  $\lambda = 248$  nm and over photolithographic methods are:

- The replacement of bulky and unreliable frequency-doubled Ar-ion lasers with industry-grade maintenance-free picosecond lasers with turn-key operation.
- The process of UV erasure by  $\lambda = 355$  nm is more resilient to dirt, grease, and residual of coating on the fibres due to the higher transmission of the 355 nm radiation as compared with the 248 nm radiation.
- A single set-up to frequency double laser sources operating over a wide range of wavelengths by simply varying the period of the UV light exposures.
- Since the erasure of  $\chi(2)$  is a multi-photon process we expect to be able to define the edges of the domains in the QPM-gratings with higher resolution.

In addition, we wanted to assess the impact of the writing wavelength on the formation of UV induced defects. In sample fabricated by erasure with  $\lambda = 244$  nm we had in fact observed significant increase of transmission losses in the periodically poled silica fibres (PPSFs) designed to generate SH in the visible spectral region. While we have now demonstrated that the formation of UV induced defects occurs irrespectively of the energy of the photons that created them, **another success of CHARMING is the discovery that exposure to visible light bleaches the UV-induced defects without affecting the nonlinearity**, thereby increasing the efficiency of PPSFs devices aimed at generating SHG at 500-600 nm

A completely new set-up for the periodic erasure was built at ORC for the CHARMING project (Figure 4 - left). It consists of a frequency-tripled Nd-YVO4 mode-locked laser, and delivers onto the uniformly poled fibre a 200 kHz train of 8 ps pulses, focused to a  $10 \times 100 \mu\text{m}^2$  spot size with a total fluence of  $200 \text{ J/cm}^2$ . The erasure of the nonlinearity is accomplished by a spatially-periodic irradiation of the fibre core with intense UV laser pulses. Laser induced free-carrier generation by multi-photon ionization causes the screening of the frozen-in field in the laser irradiated regions. In practice, we expose the uniformly poled fibre core to side illumination from the radiation at  $\lambda = 355$  nm.



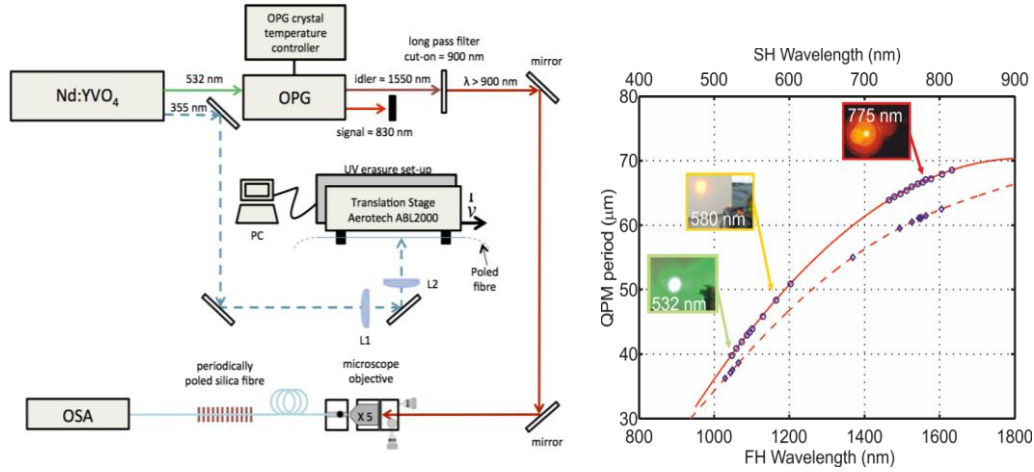


Figure 4: (left) Experimental set-up for the inscription of the QPM-grating in the induction-poled fibre by 355 nm erasure. L1 and L2 are cylindrical lens of focal length  $f = 500$  mm and 85 mm respectively used to produce a spot size on the fibre of  $10 \times 100 \mu\text{m}^2$ . The optical setup used for the SHG nonlinear characterisation of the periodically poled fibre is also shown. (right) Dependence of the QPM period on the fundamental wavelength for the (solid line) Ge-doped fibre and the (dashed line) Al-doped fibre. (Blue symbols) Experimental data points each corresponding to fabricated PPSF devices. Lines are polynomial fit to the experimental data.

One of the main challenges in CHARMING was the frequency doubling of gain-switched diodes of limited tunability. As opposed to photolithographic methods, our laser-based approach to achieve periodic UV erasure, greatly eases the task of matching the period of the QPM grating to the emission wavelength of the fundamental source; a condition that can be challenging to meet for gain-switched diodes of  $\sim 1$  nm limited tunability and with device acceptance bandwidths of  $\sim 0.2$  nm (e.g. 20 cm PPSF designed for  $\sim 1.1 \mu\text{m}$ ). The slope of the QPM period dispersion curve,  $d\Lambda(\lambda)/d\lambda \sim 0.075 \mu\text{m}/\text{nm}$  near  $\lambda = 1.1 \mu\text{m}$  (Figure 4(right)), reveals that an error of only 15 nm in the QPM period,  $\Lambda$ , is sufficient to cause a 0.2 nm mismatch between the quasi-phase matching wavelength and the laser emission wavelength.

With the procedure established in the project CHARMING, we are able to routinely achieve such tight tolerances!

The optimisation of the QPM-grating fabrication parameters such as the fluence required to achieve a complete erasure of the non-linearity in the exposed domains strongly relies on a clear understanding of the physical process behind UV erasure. **During CHARMING the collaboration between ORC and FORC proved that UV erasure is due to laser-induced free carrier generation by multi-photon ionization causing the screening of the frozen-in field in the laser irradiated regions.** The process has been described in deliverable 4.5. The main results summarized here is that:

- The decay of the nonlinearity under the laser exposure follows:  $\chi^{(2)}(t) = \chi_o^{(2)} / (1 + \alpha I^k t \chi_o^{(2)})$  where  $I^k$  is the pulse intensity and  $k$  the number of photons required by the process of multi-photon ionization,  $t$  is time and  $\chi_o^{(2)}$  is the value of the non-linearity at  $t = 0$ .
- The erasure by  $\lambda = 355$  nm is a 2-photon process in Ge-doped fibres and a 3-photon process in Al-doped fibres.

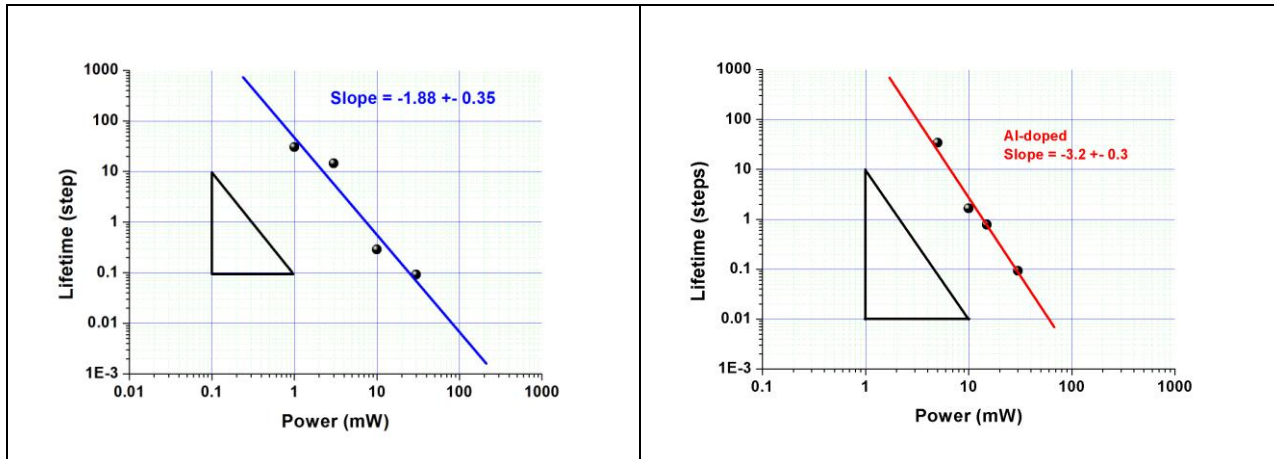


Figure 5: Lifetime dependence on erasing power of 355 nm radiation for (blue) Ge-doped fibre and (red) Al-doped PPSF

Based on the findings above we were able to develop a procedure to find the minimum laser fluence required to achieve optimum contrast  $\chi^{(2)}$ -gratings in a single scan. It relies on writing a QPM-grating multiple times at low fluence and record the SHG efficiency of the frequency doublers at each stage till a maximum or a plateau is reached (Figure 5).

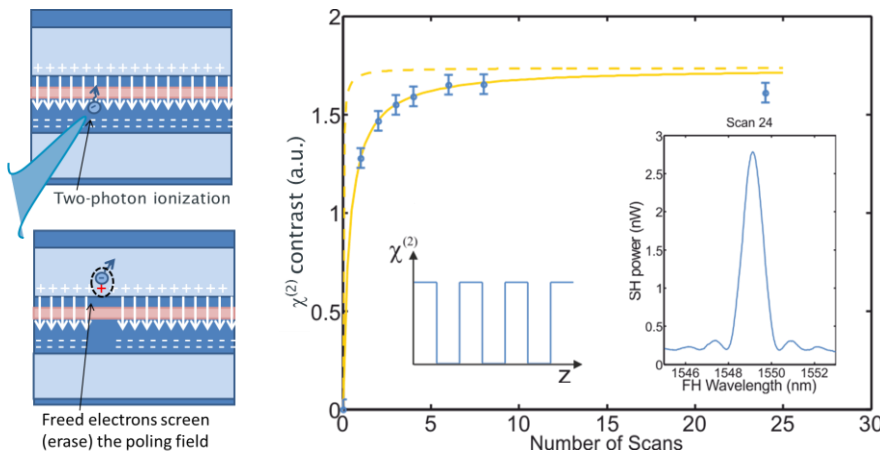


Figure 6: (Left) schematic of UV-erasure in Ge-doped fibre. A longitudinal cross-section is represented with the hole drawn in light blue, the core in pink and the poling field represented by the arrows. Free carrier electrons created by two-photon ionisation following exposure to intense 8 ps-pulses at  $\lambda = 355$  nm screen the poling field and consequently cause the decay of the non-linearity. (Right) Increase of the  $\chi^{(2)}$ -grating contrast, measured as the square-root of  $P2\omega$ , following the multiple scans of the laser beam. (insets) wavelength-tuning curve of the PPSF and schematic of the  $\chi^{(2)}$ -grating after the last scan.

Each scan only partially erases the nonlinearity so that the grating reaches the  $1/0$  contrast only after about 8 scans. Since the contrast is proportional to the square root of the SH power we can draw the graph in Figure 6. The good fit to the data give is a further confirmation that the our understanding of the physics involved, erasure of  $\chi^{(2)}$  by multi-photon ionization, is correct and described by equation  $\chi^{(2)}(t) = \chi_o^{(2)} / (1 + \alpha I^k t \chi_o^{(2)})$  with  $k = 2$  for the Ge-doped fibre. Most importantly, having understood the physics meant that we could predict the intensity to achieve  $\chi^{(2)}$ -gratings of maximum contrast with a single-scan (dashed line in Figure 6). Finally, the duty-cycle of the  $\chi^{(2)}$ -grating had to be optimized in order to compensate for the finite size of the laser beam.

**As a result the new system developed at ORC permits a very accurate inscription of long devices onto poled optical fibres.**



### 1.4.2.3. Realization of different devices with high performances demonstration

#### a) Watt level SHG in fibres at 772 nm

During CHARMING we demonstrated for the first time:

- Over 2 W of average output power at 772 nm in an all-fibre frequency doubled Er/Yb-codoped laser.
- Our results prove that PPSFs can produce and sustain multi-watt level second-harmonic generation (SHG).
- The 45% internal conversion efficiency highlights how PPSFs are particularly suited for the frequency conversion of short-pulse high power fibre laser sources.

The experiment is described in figure Figure 7. The fundamental source is a master oscillator power amplifier (MOPA) seeded by a narrow linewidth (100 kHz) tunable external cavity laser. Stimulated Brillouin scattering (SBS) in the first amplifier (FA1) is suppressed by phase dithering the seed signal with an electro-optic phase modulator (Phase EOM). Pulses of 480 ps at 5 MHz repetition rate are produced via a pair of electro-optic intensity modulators (EOM 1 and EOM 2). The two EOM and the narrow-band tunable filter (TBF) placed in between the 3 amplifiers serve the purpose of minimizing the intra-pulse CW component both in the temporal domain, by providing ~40 dB extinction ratio between pulses, and in the spectral domain, by filtering any out-of-band ASE. Additionally, a fibred polarization beam splitter filters out the ASE generated in the orthogonal polarization direction. Finally, the signal is amplified with a 3.5-m, backward-pumped, Er/Yb-codoped power amplifier (FA4). The PPSF is directly spliced to the delivery fibre which consisted of a SMF-28 spliced to 5 cm of HI1060 fibre allowing for a better mode field matching to the 6  $\mu$ m core PPSF. The passive fibre between the FA4 and the PPSF has been restricted to ~ 5 cm to mitigate the detrimental nonlinear spectral broadening due to modulation instability at high pump peak powers.

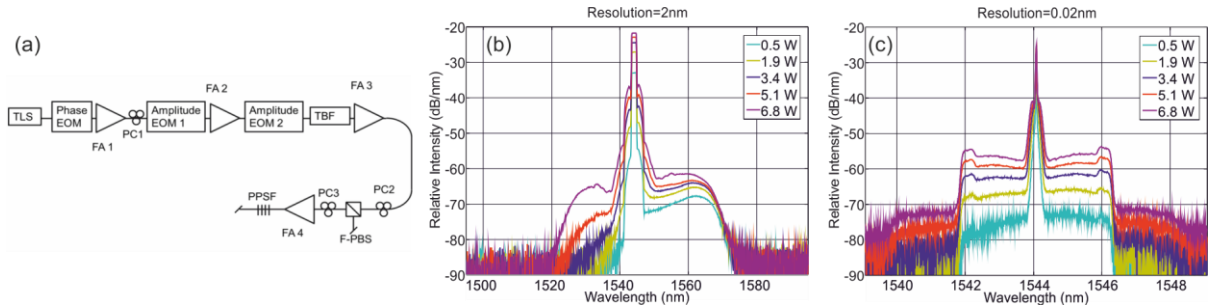


Figure 7: (a) Experimental setup of the all-fibre frequency-doubled fibre laser. (b) output FH spectra measured with an OSA at 2 nm resolution and (c) at 0.02 nm resolution.

The precautions employed to ensure high contrast pulses enable to maintain a narrow linewidth even at ~kW pump peak powers which is crucial for obtaining high conversion efficiency. Despite the apparent broadening of the output spectrum, more than 87% of the power is still contained within the central peak at the output power of 5.24 W as estimated from the spectral integration.

The PPSF devices were fabricated in the Ge-doped fibre fabricated at FORC. The samples were subsequently poled by applying 9 kV between the electrodes at an elevated temperature of 240 °C for 300 s and then cooled to room temperature. The best device in this work is 26.3 cm long with QPM period of  $\Lambda = 66.115 \mu\text{m}$  providing phase matching for 1546 nm which is close to the optimal operating wavelength of the fibre laser source. The PPSF is spliced at one end to a HI1060 pigtail resulting in ~0.4 dB loss at 1546 nm and angle cleaved at the other end.

The PPSF is initially characterized for SHG with a 5 mW continuous-wave (CW) tunable external cavity diode laser. The normalized external efficiency of the device, defined as the ratio between SH power and the square of the laser output power,  $\eta_{\text{ext}} = P^{2\omega} / (P^{\omega})^2$ , is measured to be 0.04 %/W. This value represents the highest efficiency that can be expected with the high power source in the non-depleting pump regime provided that linewidth broadening, ASE and competing third-order nonlinear effects are adequately mitigated. If splice losses are taken into account, we can calculate the

normalized internal conversion efficiency ( $\eta_{\text{int}} = 5.7 \times 10^{-2} \text{ \%}/\text{W}$ ) from which an effective  $\chi(2)$  of 0.1 pm/V can be derived. The acceptance bandwidth at FWHM is 0.66 nm for the 26.3 cm long device.

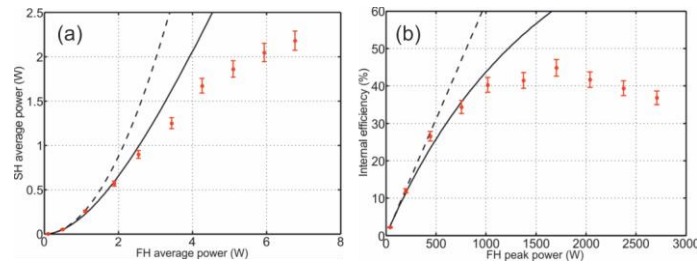


Figure 8: (a) red data points are the “external” SH output average power. Dashed line is the expected growth of the SH in the un-depleted pump approximation which is valid up to  $\sim 10\%$  conversion efficiency. Solid line is the expected SH growth considering pump depletion (b) Internal conversion efficiency.

The average second-harmonic (SH) power grows monotonically with increasing fundamental harmonic (FH) power following the theoretical predictions up to  $\sim 3\text{ W}$  of FH power (1.2 kW peak). The departure from the theoretical curve is caused by the amplification of modulation instability bands which were not sufficiently filtered out by the 4-nm-bandpass filter. Nonetheless, over 2 W of SH is generated at 772 nm for a FH power of 5.25W which represents an order of magnitude enhancement of the SH power ever generated in a PPSF. The highest external conversion efficiency at  $\sim 1.7\text{ kW}$  FH peak power is a respectable 40% with 45% internal or even 52% if we consider that only 87% of the pump spectrum lies within the acceptance bandwidth of the PPSF.

In conclusion, **we demonstrated a multi-watt level all-fibre frequency doubled laser at 772 nm with 45% internal conversion efficiency** by directly splicing a PPSF to the laser delivery fibre. The results demonstrate the ability of PPSF to handle high powers and confirm their validity as an alternative route to frequency doubling with crystals.

#### b) 521 nm in-fibre, frequency conversion with a gain-switched laser

To drastically improve the efficiency of all-fibre frequency doubling to the visible range, we have combined narrow-linewidth high power laser sources operating near  $1\text{ }\mu\text{m}$  and specially designed  $\sim 20\text{ cm}$  long PPSFs fabricated with sub-nm accuracy. In CHARMING we reported:

- **All fibre SHG with the highest average power of 50 mW at 521 nm and**
- **Record efficiency for PPSFs of  $0.3\%/W$ .**

The fibre laser source is based on a MOPA (Master Oscillator Power Amplifier) configuration from MULTITEL. The oscillator is a gain switched diode operating at 1042 nm which is firstly amplified by two single clad Yb-doped amplifiers before a last double clad booster amplifier. The laser delivers adjustable pulses from 0.1 to 4 ns at repetition rate from 250 kHz to 1 MHz, average power of 4 W and narrow spectral linewidth (50 pm full width at half-maximum). The output fibre is a single mode PM980 fibre allowing for a low loss splice to the PPSF device. The whole chain consists of polarization maintaining fibres that ensure a linearly polarized output.

Table 5: UV erasure parameters:

Sample	Core dopant	UV erasure Method	$\Lambda_{\text{QPM}}$ ( $\mu\text{m}$ )	L (cm)	$A_{\text{ov}}$ ( $\mu\text{m}^2$ )
S1	Al	355nm; pulsed	37.104	18	33
S2	Ge	355nm;pulsed	39.965	24	47

PPSF samples S1 and S2 are prepared for the frequency doubling of the Yb-doped fibre laser by pigtailling both ends with a polarization maintaining fibre. The splice losses are approximately 1.0 dB at 1  $\mu\text{m}$ . The input pigtail is directly spliced to the laser PM980 delivery fibre (0.8 dB splice) to realize an all-fibre frequency-doubled laser. The SH light is measured using a silicon detector. The unconverted fundamental radiation is separated from the SH signal by means of a dichroic mirror and of a bandpass filter centred at 521 nm.

For testing sample S1 the laser was operating at pulse duration of 4 ns, 1 MHz repetition rate. The laser wavelength was adjusted by temperature tuning of the seed laser diode to maximise the SHG. The highest SH power was recorded at the fundamental wavelength of  $\lambda_{\text{QPM}} = 1042.7$  nm. The FH power was gradually increased up to 1.2 W, corresponding to a FH peak power of 300 W. At this power level we obtained up to 50 mW of 521 nm laser radiation [Figure 9 (a)]. Further increase of the input fundamental power led to sample degradation as the SH power reached the record value of 70 mW. While this is by far the largest amount of SH generated in the visible with PPSF, it is evident that the SH power does not scale with the square of the FH power. Indeed, the highest external efficiency in the experiment is 5% at 212 W peak fundamental power. If splice losses are taken into account to obtain the power of FH and SH inside the PPSF device a 9.5% internal efficiency is calculated from which an effective  $\chi(2)$  of 0.06 pm/V is estimated.

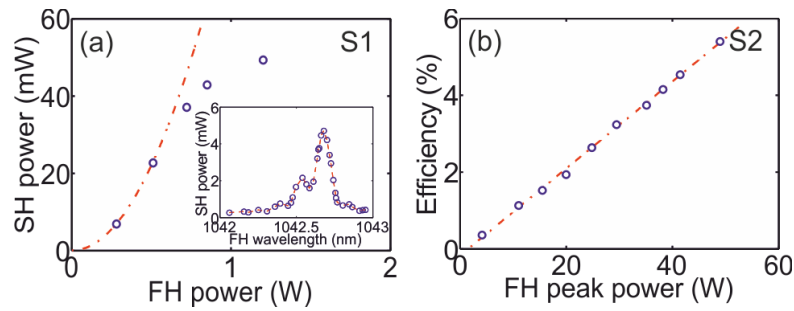


Figure 9: Sample S1: average SH power vs. FH power of the Yb-doped MOPA laser. (a)-inset: tuning curve of sample S1 obtained by varying the wavelength of the MOPA seed diode. (b) Sample S2: SHG external efficiency vs. FH peak power of the Yb-doped MOPA laser. (circles) experimental data, (line) fit to the data.

Sample S2 is more efficient than sample S1 owing to the longer length and to the higher nonlinearity we induced in the Ge-doped fibre. For FH peak power below 50 W the efficiency scales linearly with the input pump power as expected for the conversion in the non-depleting pump regime [Figure 9 (b)]. We limited our study below 50 W FH peak power to ensure stable operation over time of the PPSF. In this regime, we achieve a maximum external (internal) efficiency of 5.4% (10.3%) at only 49 W peak corresponding to  $\chi(2) = 0.1$  pm/V. The external (internal) conversion efficiency of 0.1%/W (0.3%/W) demonstrated in sample S2 is the highest ever achieved with PPSF at any wavelength (Figure 10).

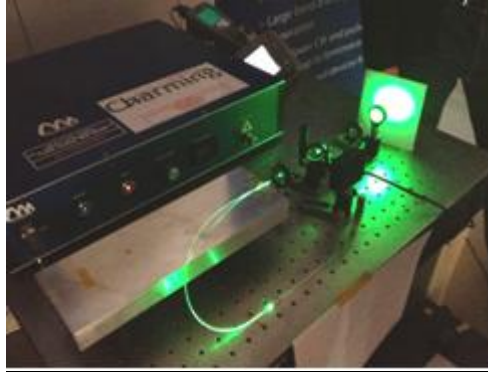


Figure 10: All-fibre laser at 521 nm obtained by frequency doubling an amplified gain-switched diode with a periodically poled silica fibre.

### c) 560 nm in-fibre, frequency conversion with a mode-lock laser

The pump source to be frequency doubled is a mode-locked (ML) laser at 1118 nm developed by MULTITEL. The repetition rate is 82.7 MHz and the pulse duration is  $\sim 20$  ps. The average output can be adjusted up to  $\sim 600$  mW which correspond to a maximum peak power of  $\sim 360$  W. For the tests with the PPSF, we used a maximum pump average power of 313 mW. Here is the scheme of the set-up used for testing the PPSF device:

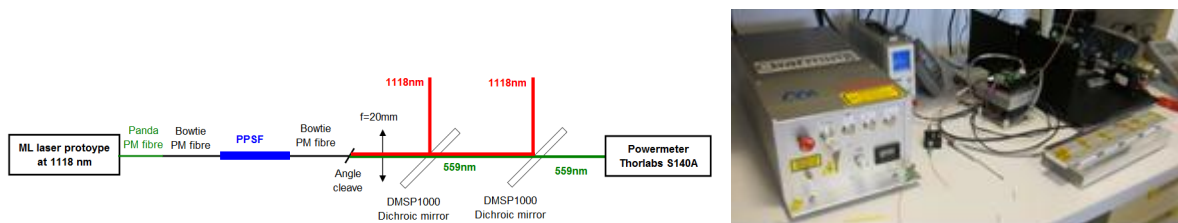


Figure 11: Scheme and picture of the set-up used for testing the 560 nm conversion of a mode-lock laser with a PPSF device.

The PPSF device was glued in a small brass groove (35 cm long) which is mounted on a temperature regulated aluminium plate. On the picture (Figure 11), one can see the brass groove mounted on the aluminium plate fixed on 4 Peltier elements and the heatsink and the ML laser prototype on the left, the PPSF and the temperature driver in the middle and the measurement setup on the top right. The temperature of the aluminium plate is precisely controlled with a computer, linked to the driver, thanks to a specially developed interface.

The temperature of the PPSF has been optimized with the maximum of pump power in order to maximize the power at 559 nm. Figure 12 shows the output power characteristic and the efficiency of the PPSF in function of the pump average power. For these measurements, the temperature of the PPSF was  $13.5^{\circ}\text{C}$ .

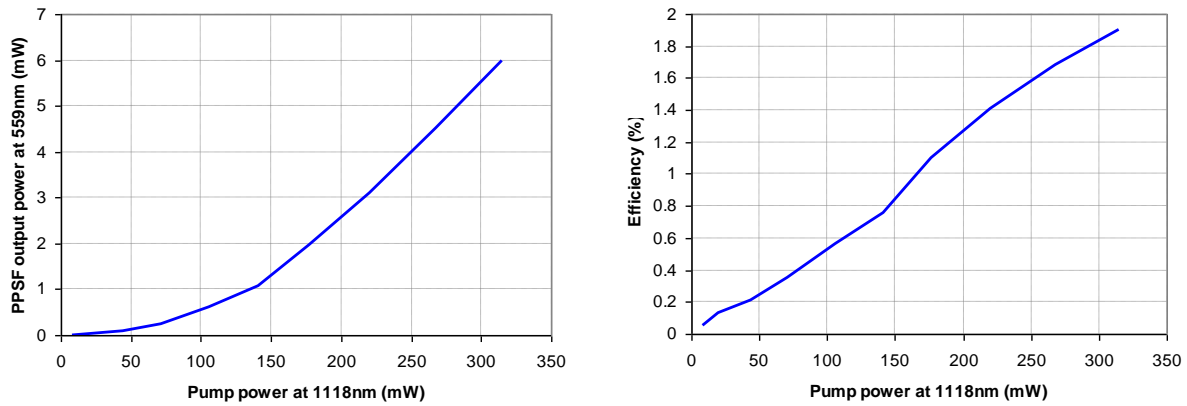


Figure 12: Power characteristic and efficiency of the PPSF

The maximum average output power at 559 nm is 6 mW with 313 mW of average pump power which corresponds to a maximum efficiency of 1.9%. We pushed the laser to its maximum to observe if the device would start decaying. We obtained more than 14 mW and did not observe any decay during a few minutes operation. We did not proceed further. **This level of average power would be sufficient for excitation sources in fluorescence imaging experiments.**

#### d) 560 nm in-fibre, frequency conversion with a gain-switched laser

For this experiment we used an active package fabricated by IXFIBER for controlling the temperature of the PPSF devices. The laser source was based on a Gain-switched module from NANOPLUS/PICOQUANT and an Ytterbium amplification stage from MULTITEL. A picture of the PPSF aluminium package designed by ixFiber for active temperature regulation and a scheme of the set-up are given below:

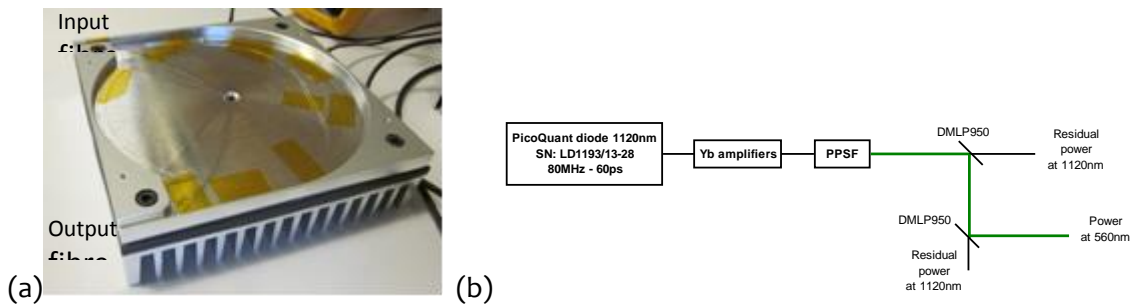


Figure 13: (a) Picture of the PPSF device in its aluminium packaging box, (b) scheme of the PPSF devices testing set-up.

Two PPSF samples have been tested, one uniform 300 mm long PPSF and one chirped 300 mm long PPSF with a spectral acceptance bandwidth of 0.5 nm. The first results given here were obtained with the uniform grating.

We have limited the laser input power in order to generate between 5 and 10 mW of SHG output power at 560 nm. In fact, this level of power is sufficient for the targeted application (excitation in STED). With 350 mW of power at 1120 nm, we obtained up to 8 mW (efficiency of 2.3%) of power at 560 nm just after the start of the experiment. A long term measurement of the power at 590 nm has been done just after the start in order to see the power stability and the decay of the PPSF. The result of this measurement is presented below:



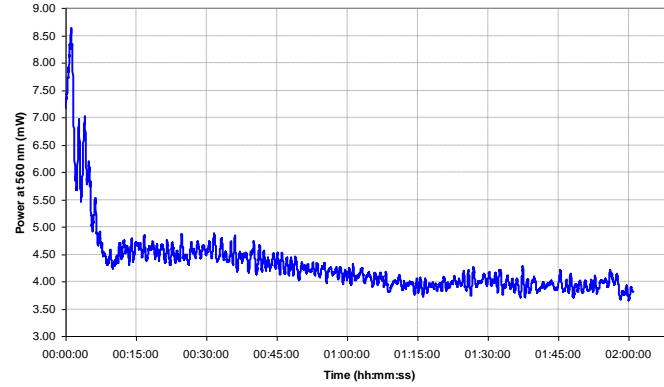


Figure 14: Variation of the PPSF SHG conversion in time.

One can see that there are some oscillations and a fast decrease of the power during the first 10 minutes (43% decrease). We assume that these two combined phenomenon are due to the power/temperature stabilization of the pump laser at 1120 nm (oscillations) and to the decay of the PPSF (fast decrease). After 10 minutes, the power stabilizes at 4.5 mW and then only a slow decrease of the power is then observed. After 2 hours, the power is about 3.8 mW (efficiency of 1%), which corresponds to a decrease of 15% in 1 hour and 50 minutes. As we did not measure the power at 1120 nm at the same time than we measured the power at 560 nm, it is not possible to be 100% sure that the slow decrease is only due to the degradation of the PPSF. Similar results were obtained with the chirped device.

**We succeeded to reach up ~8 mW at 560 nm with both uniform and chirped gratings** with a limited pump power at 1120 nm. Note that this is not the maximum of power that we could reach with these PPSF because we have not used the pump laser at its maximum. The maximum efficiency reached with the uniform PPSF is 2.3% and 1.8% with the chirped PPSF both at the start of the experiment. Then during a period of several hours, we observed a decay of the two PPSF so the SHG power decreased of about 50% in 2h for the uniform PPSF and about 18% for the chirped PPSF.

#### e) 590 nm in-fibre, frequency conversion with a gain-switched laser

The laser source was based on a Gain-switched module from NANOPLUS/PICOQUANT and a Raman amplification stage from MULTITEL. A picture of the PPSF aluminium package designed by iXFiber for active temperature regulation, a scheme and a picture of the set-up are given below:

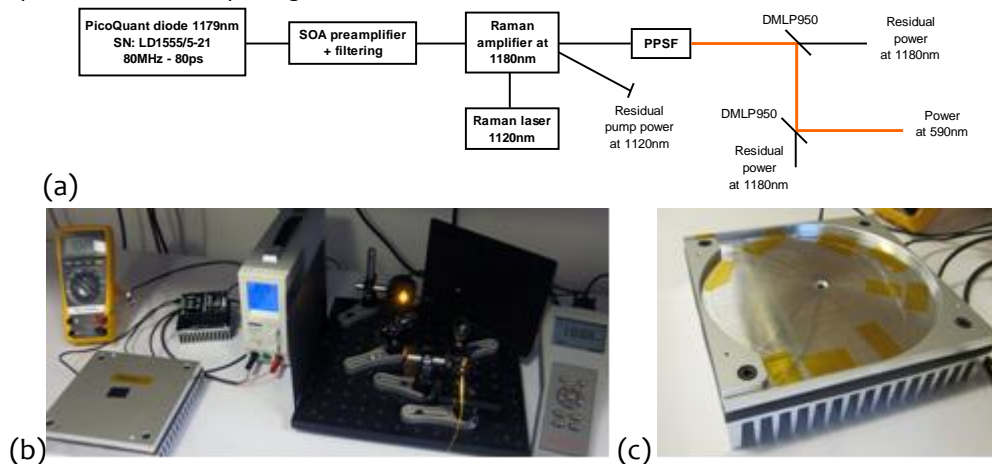


Figure 15: (a) Scheme of the PPSF devices testing set-up, (b) picture of the set-up and (c) picture of the PPSF device in its aluminium packaging box.

Two PPSF samples have been tested, one uniform 300 mm long PPSF and one chirped 300 mm long PPSF with a spectral acceptance bandwidth of 0.5 nm. The following table summarizes the results obtained with the uniform sample for the different repetition rates of the pump at 1180 nm:

Repetition rate (MHz)	80	40	20	10	5
Max average pump power (mW) (1180 nm)	1570	1170	807	580	450
Max average output power (mW) (590 nm)	22	14.3	7.9	4.45	2.62
SHG efficiency (%)	1.4	1.2	1.0	0.8	0.6
Max pulse energy (nJ)	0.28	0.36	0.40	0.45	0.52

The maximum obtained conversion efficiency was 1.4% and the maximum average power reached was 22 mW both for a repetition rate of 80 MHz. Whatever the repetition rate, the SHG efficiency increases linearly (in function of the pump power at 1180 nm) up to approximately half of the max pump power and then starts to saturate. The power characteristic at 590 nm in function of the power at 1180 nm is quite linear, whatever the repetition rate. The power at 590 nm for a repetition rate of 80 MHz has been monitored for a long period in order to detect a potential erasure of the component which could decrease its efficiency and so its output power. Below is the graph of the measured SHG power over time:

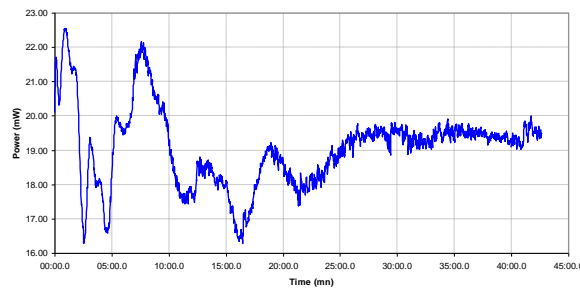


Figure 16: Variation of the PPSF SHG conversion in time.

One can see that no decrease of power has been observed during a period of 42 minutes. We can say that the fluctuations of power at 590 nm, during the first 20 mn, are due to power fluctuations of the pump at 1180 nm. After 25 minutes the power at 590 nm is stabilized at 19.5 mW. The pump laser spectral bandwidth at 1180 nm is probably too large to have the best performances with this PPSF.

The following table summarizes the results obtained with the chirped sample for the different repetition rates of the pump at 1180 nm:

Repetition rate (MHz)	80	40	20	10	5
Max average pump power (mW) (1180 nm)	1570	1170	807	580	450
Max average output power (mW) (590 nm)	30	15.2	8.5	4.5	2.59
SHG efficiency (%)	1.9	1.3	1.1	0.8	0.6
Max pulse energy (nJ)	0.38	0.38	0.43	0.45	0.52

The maximum efficiency is 1.9% and the maximum average power is 30 mW both reached for a repetition rate of 80 MHz. Whatever the repetition rate, the SHG efficiency increases linearly (in function of the pump power at 1180 nm) up to approximately half of the max pump power and then starts to saturate. The power characteristic at 590 nm in function of the power at 1180 nm is quite linear, whatever the repetition rate.

The conversion efficiency is slightly higher with this chirped PPSF than with the uniform PPSF but only for repetition between 20 and 80 MHz. The maximum power/efficiency is reached for a repetition rate of 80 MHz and is 30 mW/1.9%. During a period of ~4h, we observed a decrease of the power at 590 nm from 30 mW to 18 mW and the decrease seems not yet stabilized. Contrary to the one obtained with the uniform PPSF, the output spectrum shape of the chirped PPSF depends on the repetition rate.



We succeeded to reach up to 30 mW (1.9% efficiency) at 590 nm by second harmonic generation in periodically poled silica fibres. We tested two different PPSF, one uniform 300 mm long PPSF and one chirped 300 mm long PPSF with a spectral acceptance bandwidth of 0.5 nm. The maximum output power and efficiency has been reached with the chirped PPSF but a decay has also been observed with this PPSF after approximately 4 hours of use.

#### f) Increase of efficiency: concatenation of devices

In this section we report on 2 times efficiency enhancement for the frequency doubling of  $\sim 1.5 \mu\text{m}$  radiation by using two 30 cm long PPSFs spliced one after another. Experimental results are described here after.

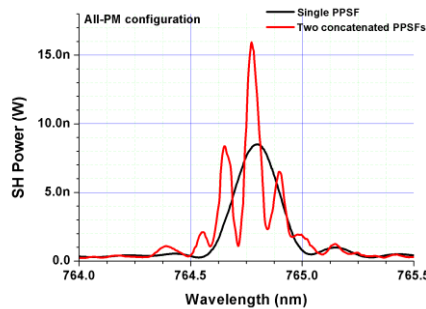


Figure 17 : SH spectra of a single PPSF (black) and of two concatenated PPSFs (red). The length of each PPSF is 30 cm, the distance between PPSFs is 30 cm. Experiment is carried out in all-PM configuration which resulted in excellent stability of the spectrum and in improved maximum SH power both in single and in concatenated PPSFs.

All the experiments with concatenation of PPSFs were carried out at room temperature. However, concatenated PPSFs are supposed to be finally used in an actively-thermalized package at temperatures of about 40 – 50 °C which could change the phase-matching conditions. So, we decided to try PPSFs phase-matching by adjusting the temperature of concatenated devices directly in the final package. This experiment is now in progress at PicoQuant. In case the temperature tuning will not be sufficient for phase-matching of PPSFs, we plan to develop optimized low-loss tapering procedure and phase-match the PPSFs before placing them into final package.

To conclude, we have demonstrated 2 times enhancement of the conversion efficiency by concatenation of two 30 cm long PPSFs. Currently, phase-matching of the PPSFs is not perfect, however we have already proved taper-induced phase-matching is possible. We have also excluded UV-induced phase-matching as it results in erasure of nonlinearity in PPSFs.

#### 1.4.2.4. Single pulse selection

Single-pulse selection using a poled fibre at multi MHz repetition rates was a goal of CHARMING. It was necessary that the devices operated single-mode at  $1 \mu\text{m}$ , were polarization maintaining, had acceptably low insertion loss, and exhibited an extinction ratio in excess of 30 dB. All these goals were achieved here. Fibres were designed for single-mode operation at  $1.06 \mu\text{m}$  with internal electrodes. An increase in nonlinear coefficients achieved during the project to above 0.3 pm/V led to the possibility of manufacturing devices with electrode lengths 25 cm instead of the original 78 cm long devices used in the beginning of CHARMING. This allowed us to reduce the RC time of devices from 28 ns to  $\sim 3$  ns. Novel electronics was designed and built to drive the components in a travelling-wave mode, which led to further improvement in the time response to the 2 ns range. Since devices were gated for a short time and discharged rapidly, the selection of single pulses from a laser running at 100 MHz was achieved. The extinction ratio measured in a PM device was in excess of 35 dB.

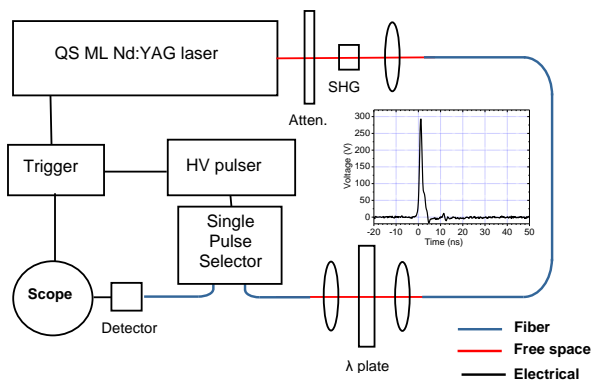


Figure 18: Single pulse selection experiment with a fibre based electro-optical device.

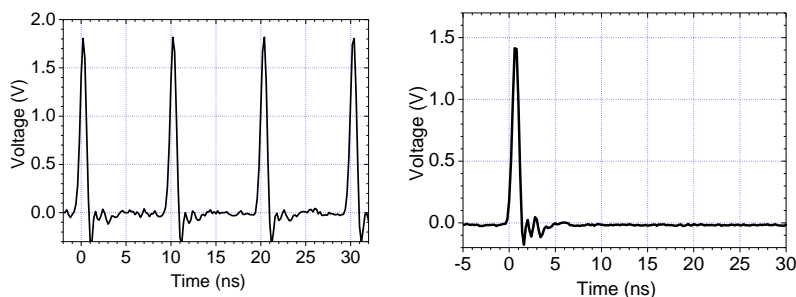


Figure 19: Single pulse selection demonstration with a fibre based electro-optical device: original pulse train on the left and selected pulse on the right.

#### 1.4.2.5. Packaging.

Two packaging approaches have been considered in the project for the long fibre periodically poled devices. The first approach (package v1) was based on a passive solution whereas the second approach (package v2) used thermoelectric active cooling.

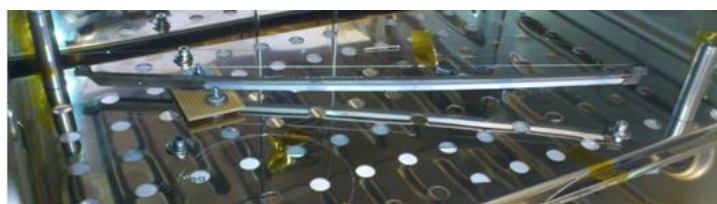


Figure 20: Picture of the athermal package assembled with a PPSF device.

The principle is the following: the linear temperature sensitivity of the in-fibre component wavelength is compensated by changing the fibre elongation. The package has been designed for different Coefficient of Thermal Expansion (CTE) materials.

The package v2 is designed to adjust and stabilize the centre wavelength of a PPSF with outer dimensions constraints for integration into the PicoQuant laser source. Specifications for the package are indicated in table below:

Parameter	Value
Maximum outer dimensions (without driver)	L x l x h : 16 cm x 16 cm x 5 cm or less
PPSF control temperature	Beyond 40 to 70 °C
Temperature stability	+/- 0.5 °C

Ambient Operating temperature	0 to 40 °C
PPSF positioning	Coiled with a radius of curvature of 7.5 cm
Other requirement	No forced-air cooling, only natural convection

Two configurations showing different ways to insert the PPSF inside the package were studied.

- Package v2.1 : PPSF is placed into a circular 5 x 5 mm U-groove machined in the copper block
- Package v2.2 : PPSF is coiled around a boss on the copper block

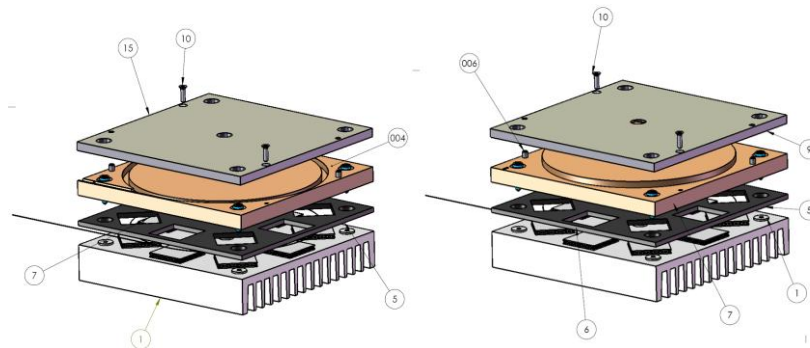


Figure 21 : The two configurations of the package v2: the PPSF is placed into U-groove (left) or coiled around a circular plate (right). The different parts are: heat-sink (1), insulation foam (5), TEC compartment (6), copper block (004 & 7), aluminium cover (9 & 15), and alignment pin (006).

### 1.4.3. WP5: Narrow linewidth pulsed laser sources

#### 1.4.3.1. New high power diodes at 1180 nm for gain-switching.

In order to achieve the results exposed before, based on different conversion experiments in periodically poled fibre devices, suitable laser sources at different wavelengths were needed. This section is related to the development of such laser sources.

During CHARMING a new epitaxy structure was designed for high power DFB laser devices. From this epitaxy DFB chips yielded an output efficiency increased by 67 % compared to the first generation that was built within the project. In order to further increase the output power and improve the farfield characteristics (thereby increasing fibre coupling efficiency), a tapered RWG design was developed and tailored to the new epitaxy. The tapered RWG design enables ex-facet output powers higher by 60 % when compared to a standard RWG design on the same material. The full width half maximum value of the laser farfield can be decreased significantly (up to 72 %) by increasing the taper angle (see Figure 22).

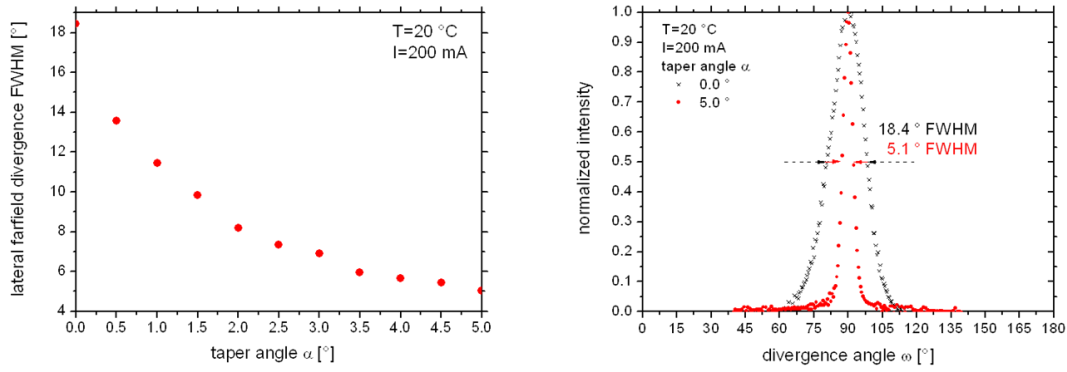


Figure 22: Relation between taper angle and lateral farfield divergence (left) and comparison of farfield distributions for 0° and 5° taper angle (right).

Using a 2° taper, the PM coupling efficiency could be increased by 26 %. Figure 23 shows the emission spectrum and ex-fibre output power of one such PM-coupled device. Other PM-coupled devices with tapered RWGs have been characterized by partner PQ in gain-switched mode. Compared to a first generation device the ex-facet peak power is increased by a factor of 7.25, the average power is higher by a factor of 7.5. Additionally the spectral width in gain-switched mode is reduced by 66 % (see

Table 6).

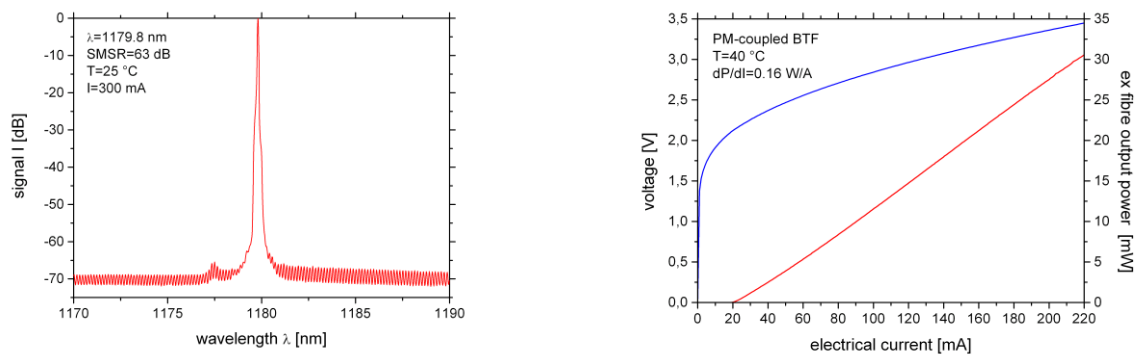


Figure 23: Emission spectrum (left) and ex-fibre output power (right) of PM-coupled 1180 nm laser device.

Table 6: Gain-switched performance of first generation laser and tapered RWG laser.

	package	cavity length	pulse width	peak power	average power	spectral width
1 <sup>st</sup> generation laser	TO5 can	900 μm	60 ps	16.7 mW (ex-facet)	80 μW (ex-facet)	0.3 nm
Tapered RWG laser	PM-BTF	1200 μm	63 ps	48 mW (ex-fibre) =>121 mW ex-facet	240 μW (ex-fibre) => 602 μW ex-facet	0.1 nm

#### 1.4.3.2. New gain-switched devices at 1180 nm.

The latest tested 1180 BFY packaged laser diode showed very good performance and is in line with the expectations at the beginning of the project. A pulse energy of 3 pJ and spectrally narrow emission make the diode well suited for upcoming amplification experiments.

In summary, the main goals have been well achieved and for the final designs of the 1120 and 1180 laser diodes. The pulsing characteristics are already very comparable to state of the art laser chips at other wavelengths (e.g. telecom 1550nm or 1064nm) from different commercial vendors.

Manu- facturer		Housing	Nominal Lambda	Rated cw Power	Shortest pulse- width	pulse energy	Wavelength pulsed	Spectral width pulsed
NP	374/1-16	TO5	1180	10mW	163 ps	7 pJ	1178 nm	0.2 nm
QD-Laser		BFY+ISO	1120	50mW	93 ps	3 pJ	1115.5 nm	0.5 nm
NP	296/10-12	TO5	1120	20mW	176 ps	3 pJ	1118.0 nm	0.6 nm
NP	1124/6-32	TO5	1179	24mW	68 ps	1 pJ	1179 nm	0.3 nm
NP	1193/2-28	TO5	1121	55mW	44 ps	5 pJ	1121 nm	0.6 nm
NP	1193/9-5	BFY	1120	24mW	42 ps	7 pJ	1117-1118nm	0.4 nm
NP 900µm	1193/14-24	TO9	1124	53mW	50 ps	23 pJ	1121.3-1121.7	0.35 nm
NP 900µm	1193/14-25	TO9	1123	38mW	45 ps	32 pJ	1120.4-1121.1	0.35 nm
NP 450µm	1193/17-25	TO9	1123	40mW	43 ps	13 pJ	1120.2-1121.5	0.45 nm
NP 450µm	1193/17-26	TO9	1122	45mW	46 ps	13pJ	1119.4-1119.6	0.40 nm
NP	1193/11-6	BFY+ISO	1120	23mW	70 ps	3 pJ	1119.2-1119.6	0.45 nm
NP	1137/11-6	TO9	1064	65mW	83-140ps	~10pJ	1063.3-1163.5	Weak DFB
NP	1555/5-20	BFY	1180	27mW	80 ps	1 pJ	1179 nm	0.3 nm
NP	1555/5-21	BFY	1180	27mW	63 ps	3 pJ	1180 nm	0.1 nm

Figure 24 : Summary of measured laser diodes characteristics. BFY-Butterfly housing including fibre coupling. TO5 and TO9 housing have free space output. TO5 and Butterfly housing come with TEC and NTC for thermal stabilization. The pulse energy is measured at output (free space or fibre output for Butterfly housing)

#### 1.4.3.3. Raman amplification at 1180 nm.

This part has been an important challenge in the project. As explained in section 1.4.1.1, we gave up bismuth fibre amplification option because of the too large pump power and fibre length required for relatively low gain at room temperature. This would have resulted as a very cumbersome and expensive multi-stages amplification system.

As a consequence, we investigated Raman amplification as a back-up solution. The Raman amplifier is based on a single pass configuration. The basic design of the Raman amplifier is the following:

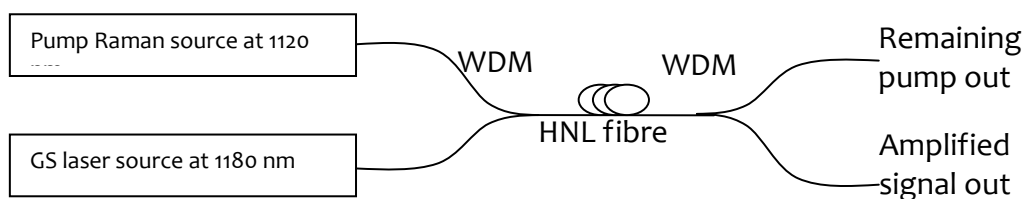


Figure 25 : Scheme of the Raman amplifier at 1180 nm.

The pump source delivers 19 W at 1122 nm. The Raman amplifier contains only 50 m of nonlinear fibre. The following figure shows the maximum amplifier average output power in function of the repetition rate:

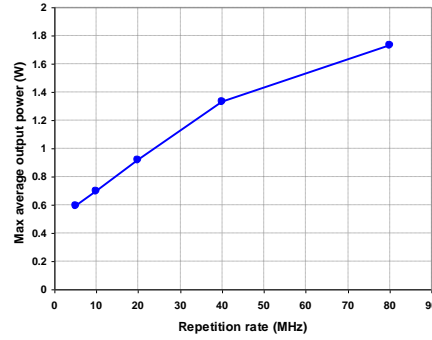


Figure 26 : Raman amplifier average output power in function of the input repetition rate of the gain-switched laser source at 1180 nm.

As we can see we were able to amplify beyond the Watt level. During amplification there can be noise added between the pulses due to spontaneous emission. As the most important parameter for efficient subsequent frequency conversion is the available peak power within a certain acceptance bandwidth, we made this calculation. The two following figures show the output peak power (considering the measured pulses shapes for each rep. rate) and the maximum pulse energy in function of the repetition rate:

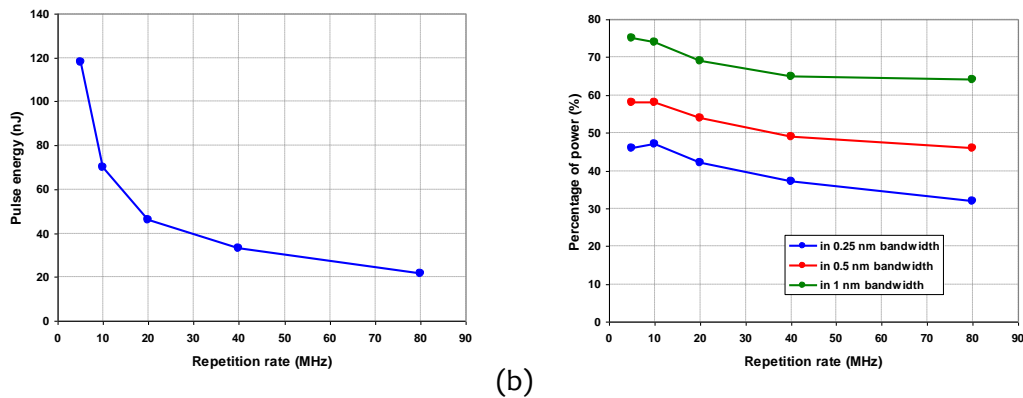


Figure 27 : (a) Raman amplifier output pulse energy and (b) percentage of power in 0.25, 0.5 and 1 nm bandwidth in function of the input repetition rate of the gain-switched laser source at 1180 nm.

After measuring the spectrums at full power for all the repetition rates, we have calculated the percentage of power in three different spectral bandwidths centred on the maximum spectral peak. The following table summarizes the results:

Repetition rate (MHz)	80	40	20	10	5
Max average output power (W)	1.73	1.33	0.92	0.7	0.59
Max residual pump power (W)	11.2	11.3	11.8	12	12.2
Max peak power (W)	259	223	252	335	552
Max pulse energy (nJ)	22	33	46	70	118
Percentage of power in 0.25 nm bandwidth (%)	32	37	42	47	46
Percentage of power in 0.5 nm bandwidth (%)	46	49	54	58	58
Percentage of power in 1 nm bandwidth (%)	64	65	69	74	75



## 1.4.4. WP6: Devices and lasers integration

### 1.4.4.1. Confocal and STED experiments.

A gain-switched 559 nm laser source based on Nanoplus 1118 nm laser diode and iXfiber amplifier fibre was used for integration into a confocal microscope at PicoQuant. Conducted experiments proved this source is suitable for time-resolved spectroscopy and advanced methods such as dual colour FCS (fluorescence correlation spectroscopy) or PIE FRET (pulsed interleaved excitation Förster resonance energy transfer).

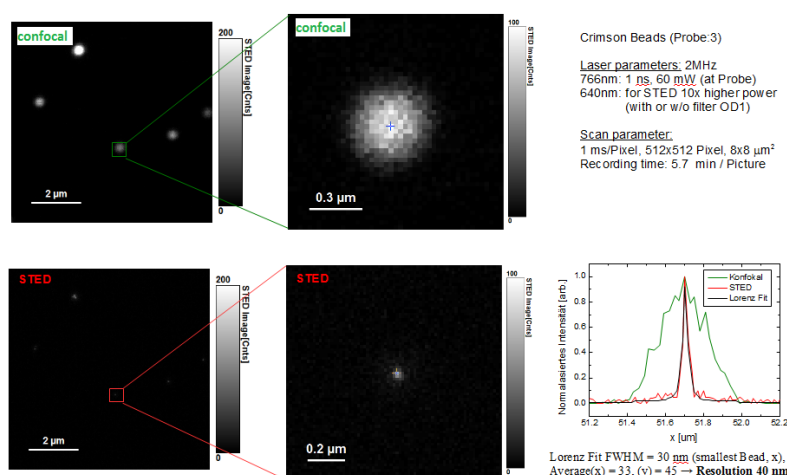


Figure 28: Comparison of confocal and STED resolution with crimson beads. Resolution enhancement from  $\sim 300$  nm down to 40 nm was achieved with 1 ns long STED pulses at 766 nm.

The main goal for D6.2 was the Integration of a high power source at 766 nm for a super-resolution microscopy system. A several 100 mW laser source at 765 nm was integrated at PicoQuant in a newly developed platform for super-resolution microscopy or also called Nanoscopy. The concept of STED (stimulated emission depletion) was successfully demonstrated with an enhancement in resolution from 300 nm down to 40 nm compared to classic confocal approaches.

The new STED microscope platform including the pulsed 765 nm laser was presented to public during the “20th International Workshop on Single Molecule Spectroscopy and Ultra Sensitive Analysis in the Life Sciences” in September 2014. This was followed by market launch at the end of 2014.

An upgrade of the existing laser sources to different frequency conversion scheme (i.e. PPSF) is possible at any time once long term stability and performance is confirmed. The integration into microscope systems is completely independent from type of the SHG signal generation, so that the general prove of concept with the newly developed pulsed sources in this project could already be demonstrated.

## 1.4.5. WP7: Demonstration

### 1.4.5.1. Fibre devices integration with gain switched lasers

We have demonstrated the possibility to integrate periodically poled SHG devices with gain switched diodes both at 1120 nm and 1180 nm. The obtained performances could be sufficient for Excitation signals in STED experiments.



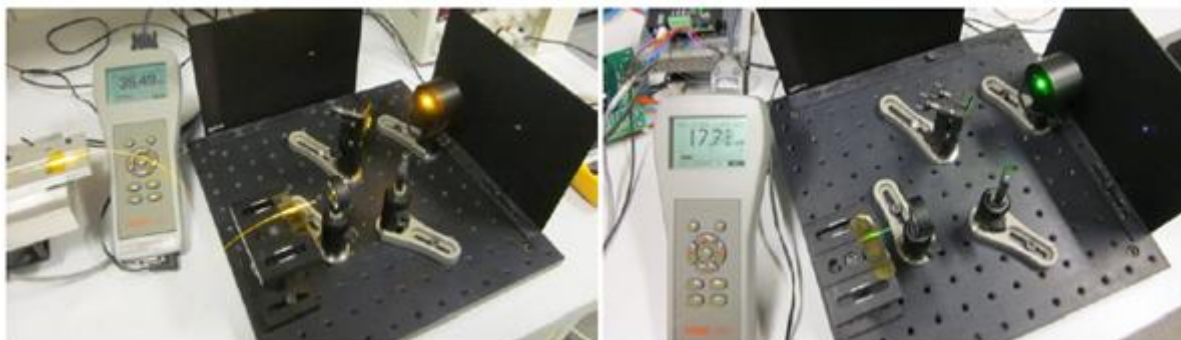


Figure 29: Picture of SHG experiments with gain switched laser diodes and fibre PPSF devices at 590 nm (left) and 560 nm (right)

For depletion applications, **we were able to reach 200 mW at 590 nm** with a gain-switched module fibre coupled to a PPLN SHG device. Finally, for Tryptophan imaging application we have been able to generate 0.6 mW at 295 nm:

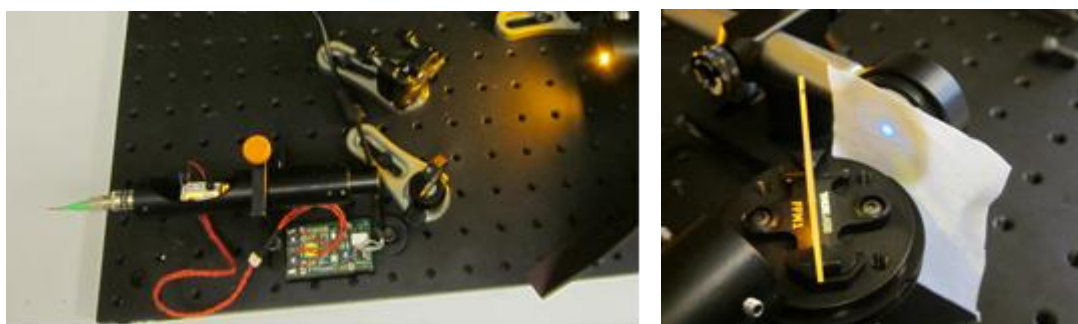


Figure 30: Picture of SHG experiments with gain switched laser diodes and PPLN/BBO crystals at 590 nm (left) and 295 nm (right)

**All these results are compatible with the applications targeted in the project.**

#### 1.4.5.2. Demonstration of 559 nm pulsed source for FLIM applications

One major application of a 559 nm pulsed laser source is the identification of FRET artefacts. In order to quantify measurements with involved Förster Resonance Energy Transfer (FRET), it is helpful to determine the relative quantities of donor and acceptor intensity and the actual cross talk between donor and acceptor channel and other measurement artefacts, which mainly depend on the relative concentrations, used intensities and filter sets for one given setup. One way of checking the quality of the sample is using pulsed interleaved excitation, shown in Figure 5. If a FRET sample is excited with two different colours consecutively, a matrix of four different images can be recorded, depending of excitation and detection channel. This way, cross talk and direct excitation can be directly identified. Furthermore, the fluorescence lifetime information for each component of the matrix is available in that case, allowing for a combined time-resolved and spectrally resolved FRET-analysis.

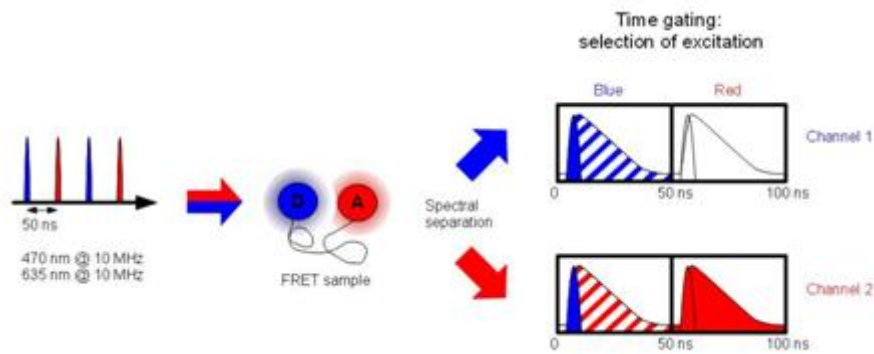


Figure 31: Principle of dual colour pulsed interleaved excitation (PIE) to identify FRET artefacts

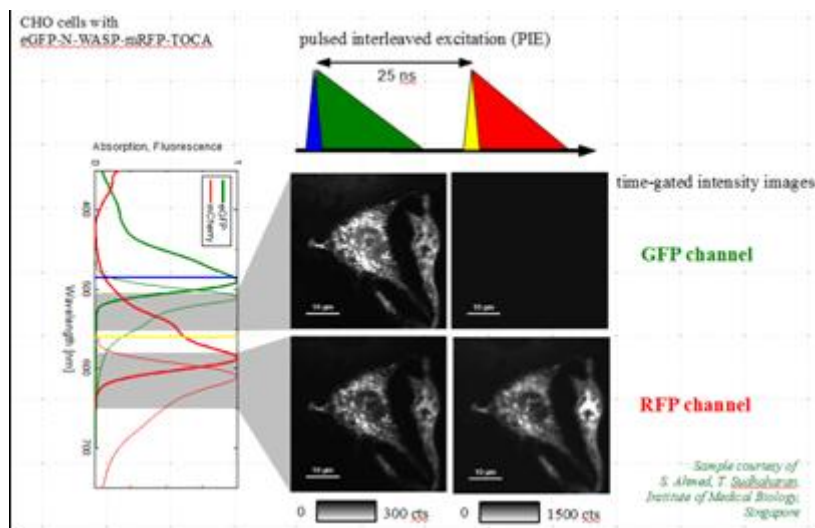


Figure 32: FRET imaging with standard 485nm and CHARMING 559nm laser head with PIE. GFP and RFP represent the green fluorescent protein (e.g. eGFP) and red fluorescent protein (e.g. mCherry) respectively.

#### 1.4.5.3. Demonstration of 266 nm pulsed source for tryptophan spectroscopy

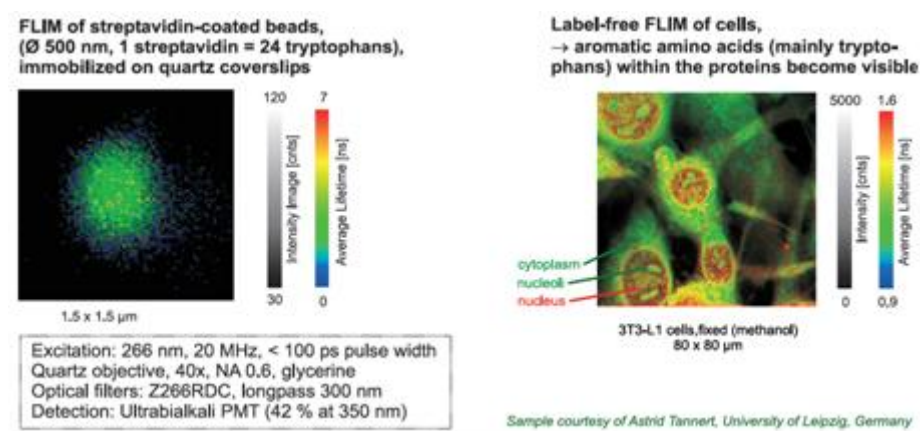


Figure 33: Intrinsic fluorescence of tryptophan-containing proteins.

Extension of the excitation wavelengths into deep UV, e.g. 266nm, grants access to the intrinsic fluorescence of tryptophan-containing proteins. Label-free FLIM with biological cells becomes feasible where the aromatic amino acids within the proteins become visible.

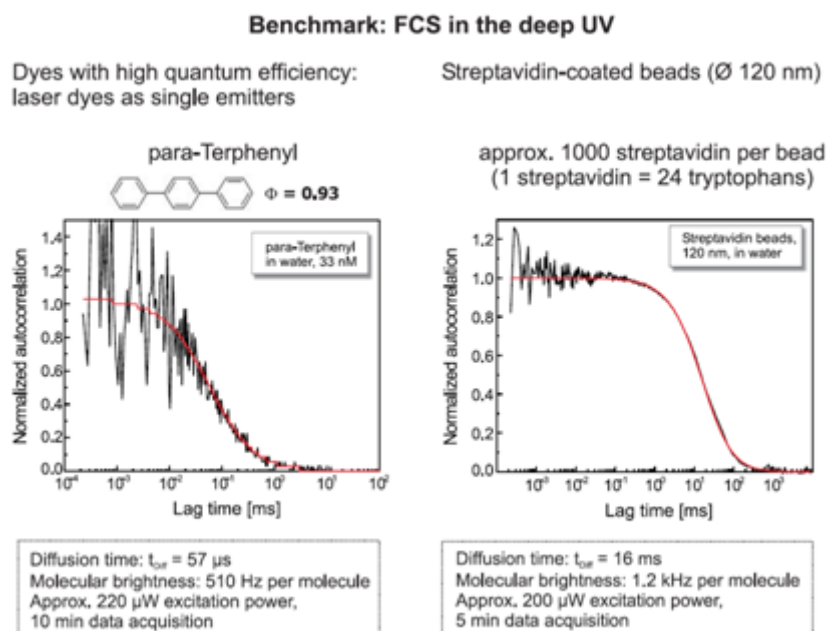


Figure 34: Fluorescence Correlation Spectroscopy (FCS) benchmark test shown with organic fluorophors excited at 266nm

Figure 34 shows a benchmark result obtained with a 266 nm pulsed source developed during the project performing FCS.

#### 1.4.5.4. Demonstration of 355 nm pulsed source for fluorescence spectroscopy

The 355nm pulsed source is based on a 1064nm gain-switched Seed and two-stage fibre amplifier. A cascaded frequency conversion starting with SHG to 532nm and subsequent sum-frequency mixing of fundamental and second harmonic creates 355nm pulsed signal in the mW average power range.

After integration into a prototype housing, the laser was tested at PicoQuant's time-resolved fluorescence spectrometer FT300. A sample measurement shown in Figure 35 indicates full suitability for various applications. Both pulse shape and spectral properties match the requirements for clean fluorescent signal detection and software analysis.

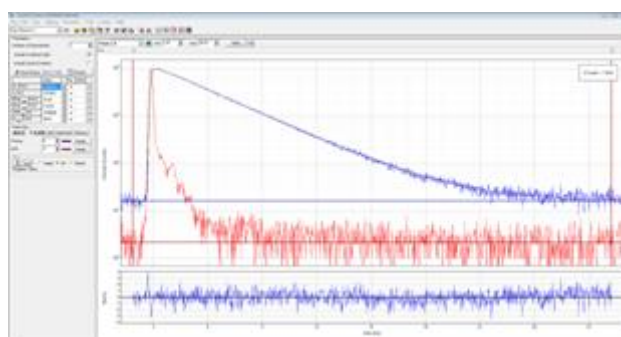


Figure 35: Coumarin 6 in EtOH excited at 355nm at 20MHz. Detection at 505nm. Fitted lifetime of 2.53 ns, in accordance with literature. The measurement was performed in a FT300 fluorimeter equipped with a TH260-P as TCSPC board and a PMA-192 PMT as detector.

## 1.5. General conclusion and potential exploitable results

The project CHARMING led to various records and new results in the field of electro-optic and periodically poled fibre devices for optical modulation and second harmonic generation in fibre.

This project permitted to increase the knowledge on the fabrication of such devices and, with the increase of performances, also permitted to evidence some limits.

As a consequence, although the fibre based technology for SHG could certainly be applied for specific applications like low power visible generation for excitation purposes in STED or high power conversion of narrow linewidth lasers at 1550 nm and also quantum cryptography, the technology is not sufficiently flexible at the moment.

This lack of flexibility prevents any plans for launching a spin-off activity on this topic and non of the aforementioned potential applications is large enough to justify a sufficient economic activity.

In order to be able to address a sufficiently large market fibre based SHG devices must gain in flexibility, i.e. be less sensitive to laser parameters like bandwidth and be more robust (problem of decay). The main impact of the project CHARMING related to this topic is scientific and technological with an important improvement of the state-of the art in the field.

The electro-optic fibre devices developed in the project have shown a higher level of maturity but will need, as for SHG fibre devices to compete with existing and well established technologies like electro-optic and acousto-optic based solutions.

Regarding laser sources, this is certainly where the closest to market solutions of the project are. Indeed the improvements of DFB laser sources will naturally lead to new products in Nanoplus portfolio. All the gain-switched sources in the UV and visible, based on standard conversion schemes, developed in the project will lead to new products from PICOQUANT. A particular attention in this respect to the 590 and 295 nm wavelengths that are accessible thanks to the developments done in the project CHARMING and that can lead to interesting exploitation routes.

## 1.6. Potential impact

In the project CHARMING there are two aspects that have to be taken in consideration for what concerns the exploitation potential:

- The biomedical imaging systems (STED, FLIM, FCS and others) that require new wavelengths with specific pulse parameters.
- The stand-alone devices like the diode lasers and in particular the new fibre components like the PPSF modules for SHG or for pulse gating.

In the first domain, biomedical imaging, new gain-switched lasers sources at different wavelengths with various potential applications are now achievable thanks to the project CHARMING (like 766, 590, 560, 355, 295 and 266 nm). Potentially these new wavelengths are sufficiently interesting as such to justify for a large interest and future products. For all the visible wavelengths (560, 590 and 766 nm) an all-in-fibre approach will be a benefit from the fabrication point of view (easiness of assembly) and for the robustness of the system in a long term operation (no free space optics). Nevertheless, given the progress on the gain-switched lasers and amplifiers done in the project CHARMING, given the potential interest of the wavelengths we already have at reach and finally given the low visibility we have for the moment on the all-fibre devices long-term reliability and final performances; we believe that an exploitation strategy based on first introduction of the new achievable wavelengths in the market and then integrating later the in-fibre devices when the technology will be more mature is the most realistic and efficient way to proceed. We can already expect from the developments achieved in the project a large exploitation potential in the biomedical field.



For the second category of exploitable results, i.e. the stand-alone products; these devices are not limited to the biomedical field. The developments done by Nanoplus on the laser diodes are very promising and not limited to the delivery of new diodes at 1120 and 1180 nm to PICOQUANT. The new laser designs and the implementation of an in-house PM coupling unit will be transferable achievements to other wavelengths and will then impact on the general turnover of the company. Concerning the in-fibre devices, their applications are not limited to the bio-medical field. Indeed, having as much in-fibre functions as possible is always the preferred solution for laser developers, for a question of handling, mechanical stability and reliability. It is important to develop such new approaches in Europe. When one looks at the status of the fibre components fabrication in the world, most of the “simple” in-fibre or fibre coupled functions (isolators, couplers, WDM) are fabricated out of Europe. The main fibre coupled devices remaining in Europe are the electro-optic and acousto-optic modulators (e.g. Photline, AA group for instance) and the SHG PPLN crystals (e.g. Covision, Altechna and Goosch and Housego that recently released a very preliminary version of a fibre coupled PPLN device...). All these fibre functions that require a strong know-how have better chances to face the foreign competition. We have made important progress in this technology (new erasing wavelength at 355 nm, poling of new type of fibres, understanding of the decay mechanism, possibility to pole with removable metallic electrodes, high voltage poling, concatenation of devices...).

All this accumulated knowledge will give a leading position to European research and will permit to develop future products:

- IR laser diodes,
- Fibre SHG and pulse-picking devices for fibre lasers,
- High voltage field measurement,
- Quantum communications

### **1.6.1. Potential markets:**

#### **1.6.1.1. Biomedical applications**

The major markets are in molecular and cell biology. Here (confocal) microscopic methods play a dominant role for imaging. Also neuro-sciences show an increasing demand especially for high resolution microscopy using the STED method. The UV wavelengths are especially important for protein studies and imaging intrinsic fluorophores like aminoacids, NAD, NADH, FAD etc. Also time resolved fluorescence spectroscopy of these biomolecules show an increasing demand for shorter excitation wavelengths. Beside the “Bio” market there are always customers working in more basic research at universities. Typical applications are material sciences, solar cells and quantum optics research.

The initial exploitation plan for PQ for the CHARMING project targeted an expected additional annual turnover of up to 5 Mio €. Beside the commercial exploitation, PQ wanted to use scientific results from the CHARMING project to strengthen its high scientific reputation by presenting the results as talks or posters at leading international conferences like BIOS/Photonics West, FOM or the annual Single Molecule Workshop.

Both goals seems still possible or have been even partly reached. As shown below the expected additional annual turnover containing products developed inside CHARMING is estimated to be approx. 4 Mio € for 2017. It is typical for PQ that a new technology needs 3 years before being an effective contributor to the turnover.

As PQ's developments and sales are mainly driven by recent customer needs in the life sciences, a certain change in the distribution of the turnover to individual applications can be found here compared to the expectations given in the DOW. However the remarkable result is, that although the distribution is different than expected the total amount is very similar. The small reduction in turnover is due to the missing stability of an all fibre approach as initially planned as well as missing the high power 1180nm solution at the end of the project.

To this list should be added now the 590 nm (high power) and 295 nm band that are now possible with the availability of the high power Raman amplifier developed in the project by MULTITEL.

### **1.6.1.2. DFB diodes**

DFB diodes from 600 to 1200 nm are of particular interest for bio-medical spectroscopy applications, especially the study of red fluorescent proteins in the context of intra-molecular dynamics. A narrow and stable spectrum is required for precise spectroscopy measurements and also in the case of the diodes for subsequent frequency doubling to 560 or 590 nm. The need for 560 and 590 nm light sources is detailed further in sections 3 and 4 where the corresponding applications are described. Additionally, as further explained in section 5, there is a market for Gain-Switched lasers emitting at ca. 760-780 nm. At the moment these wavelengths are reached by frequency doubling the output of 1550 nm lasers. The transfer of the design developed by NANOPLUS at 1120 and 1180 nm to the 760-780 nm range will result in the option for NP to provide laser diodes suited for gain-switching directly at the wavelengths in question, omitting the need for frequency doubling.

Market research among pre-existing customers and interested companies such as Toptica, Partec and Coherent during the first 18 months of the project indicates a keen interest in the above applications. End customers for the spectroscopy applications would mainly be bio-medical laboratories, hospitals, healthcare companies and research facilities. Based on this target clientele, annual sales will realistically amount to between 30 and 60 units per application per year for the foreseeable future, with fluorescence correlation spectroscopy and fluorescence lifetime measurement initially being the main applications. In accordance with those figures we estimate sales - after the ramp-up of serial production and upfront promotion of the products during the first six months following the project - to increase from an initial 30 lasers at a turnover of EUR 90.000 in 2015 to between EUR 225.000 and EUR 300.000 for 75 to 100 lasers in 2017.

High power combined with a narrow linewidth has always been an important request from end-users for a variety of applications. The high power laser diode design developed by NANOPLUS in the frame of CHARMING is not limited to one material system, i.e. it can be applied to most of NANOPLUS' products, currently being the only supplier covering the whole wavelength range between 0.8 – 5.2  $\mu\text{m}$ , thus adding an additional unique selling point to our product portfolio. Among the applications in question are long range absorption spectroscopy for safety and security e.g. the detection of flammable gases at industrial complexes or on oil rigs, LIDAR (Raman-, Rayleigh-, Doppler- and Differential-LIDAR), high precision laser metrology, pump lasers (EDFA, YDFA, Er:YbFA) mainly for material treatment and Laser-Guide-Stars for observatory telescopes.

The total share of semiconductor lasers in those markets amounted to USD 1210 Mio in 2013<sup>1</sup> with an estimated average growth of 5 to 7 % for the following years. Some of the applications mentioned above, long range absorption spectroscopy and pump lasers in particular, are large volume applications with a demand of several hundreds of up to a thousand units per year. Based on purchase forecasts from our customers and interested parties, like e.g. Senscient, General Monitors, Toptica and Heidenhain, we estimate sales of approximately 100 lasers at a turnover of EUR 150.000 during the introduction phase in 2015, leading to annual sales of around 1600 units per year at EUR 1.880.000 in 2019. Turnover does not increase at the same rate as units sold, as prices per laser are likely to decrease with large volumes being ordered leading to an average price of EUR 1.175 per unit.

---

<sup>1</sup>

<http://www.laserfocusworld.com/articles/print/volume-50/issue-01/features/laser-marketplace-2014-lasers-forge-21st-century-innovations.html>

#### **1.6.1.3. Athermal packaging for long fibre devices**

Athermal packaged FBGs are much less sensitive to temperature than unpackaged FBGs that show a wavelength drift of about 7.1 ppm/°C. They are suitable for applications where spectral filtering with high thermal stability is required like, for instance, amplified spontaneous emission filtering in a two-stage laser, optical add-drop multiplexing and mirrors for fibre-laser. Gratings up to 35 mm long can be inserted into 5 cm standard-length packages, nevertheless longer packages are also expected for specific applications. They address narrowband filtering, serial-FBGs in a single package, long chirped gratings or stable long-period gratings. Pulse stretching, radio-over-fibre systems are some examples of applications. Moreover, the design of the package developed in the Charming project enables to easily adjust its compensation rate to lead to a flexible solution “one package for different types of gratings”. For instance, it makes easier the compensation of various long period gratings showing a thermal sensitivity that depends on both fibre and grating period.

About 15 % of the FBG-based product sold by iXfiber are supplied with a temperature-compensated package. Most of them consists of a few centimeters long gratings. But longer gratings and serial gratings could benefit from long passive packages.

#### **1.6.1.4. Periodically poled fibre devices**

The notion of entanglement is one of the corner-stones of quantum-mechanics. In recent years the use entangled photon-pairs have been proposed for applications outside the research lab. Quantum Key Distribution (QKD) is arguably the most “mature” technology with network security solutions based on quantum technologies already present on the market (see e.g. <http://www.idquantique.com/>). In this respect the availability of a broadband source of entangled photon pairs and wavelength-division-multiplexing gives rise to the ability to distribute entangled bi-photons to multiple users.

Besides QKD, other applications are rapidly gaining consensus. Entangled photons sources are finding use also in quantum metrology and high resolution interferometry where the detrimental effects of group-velocity dispersion are mitigated by entanglement.

#### **1.6.1.5. Electro-optic fibre devices**

The total market for fibre lasers for material processing exceeds US\$ 700 M, and for marking alone US\$250 M. The main market we target is pulse-picking. Most ultrashort fibre lasers in use today for micromachining require single-pulse selection. It is very difficult to achieve ultrashort pulse generation at low repetition-rates in a stable and reproducible way directly from the laser. Therefore, laser designers use pulse-pickers for reducing the repetition-rate of their ultrashort pulse source. Pulse-pickers are also used in other markets envisaging the reduction of the pulse rates, as in CHARMING.

Another market that can be targeted with our electro-optical fibres is as fibre-based phase-modulators for applications in fibre-optical gyros, in instrumentation, telecom, and sensing (current, acoustic, intrusion sensing).

### **1.6.2. Social impact:**

The availability of laser sources developed in CHARMING is bound to bring a true positive impact for society, for biomedical research, drug discovery, cell analysis, proteomics and others. During the term of the project, one technology has already been awarded the Nobel prize: super-resolution microscope.



Laser sources at higher power level were developed to increase the resolution as well as increasing the flexibility of the sources for adaption to various biological or chemical samples. Super-resolution techniques like STED and photo-switching microscopy are just opening the doors to a truly new dimension in optical microscopy for bio-imaging. For the first time it is not only possible to really “see” the structure of cell organelles in much more detail but also to study for example the internal structure of bacteria, with a size typically far below the optical diffraction limit.

Fluorescence Lifetime Imaging Systems (FLIM) are applied in many biomedical fields. In a reference from 2007, researchers applied this technique for in vivo studies to localize tumors and detect their progression with adapted fluorophores. The work was oriented towards monitoring the efficiency of drug delivery. Their set-up included fibre beam delivery and collection in order to target endoscopic applications.

The most promising direction in this field is for safe in-vivo skin and tissue characterisation to identify tumours and other specific defects based on a lifetime assisted auto-fluorescence imaging. In recent years, several research consortia started to develop instruments for medical diagnosis for epidermal skin imaging, ophthalmology and endoscopic imaging inside living specimen.

FLIM has already been applied to monitoring of nicotinamide adenine dinucleotide (NADH), an essential coenzyme for the liver. FLIM is also used in high content drug screening, to identify potential pharmaceutical ingredients in multiplexed assays and in proteomics to improve the characterization of total protein expression maps.

As a consequence the project CHARMING will have a positive impact in our lives through the improvement of the means for diagnosis and early stage screening of various diseases.

### 1.6.3. Dissemination and exploitation tables

#### 1.6.3.1. List of scientific publications

**TEMPLATE A1: LIST OF SCIENTIFIC (PEER REVIEWED) PUBLICATIONS, STARTING WITH THE MOST IMPORTANT ONES**

NO.	Title	Main author	Title of the periodical or the series	Number, date or frequency	Publisher	Place of publication	Year of publication	Relevant pages	Permanent identifiers <sup>2</sup> (if available)	Is/Will open access <sup>3</sup> provided to this publication?
1	Soliton generation from an actively mode-locked fiber laser incorporating an electro-optic fiber modulator	M. Malmström (ACREO)	Optics Express	Vol. 20 Issue 3, (2012)	OSA		2012	pp.2905-2910		yes
2	Pulse selection at 1 MHz with electrooptic fiber switch	M. Malmström (ACREO)	Optics Express	Vol. 20 Issue 9, (2012)	OSA		2012	pp.9465-9470		yes
3	Advances and Prospects of Frequency Doublers Based On Periodically Poled Silica Fibres [invited]	C. Corbari	BGPP 2012, Conference on Bragg Gratings, Photosensitivity and Poling in Glass Waveguides	June 2012	OSA		2012			no
4	Direct generation of polarization-entangled	E. Zhu	Physical Review Letters	Accepted for publication	APS		2012			no

<sup>2</sup>

A permanent identifier should be a persistent link to the published version full text if open access or abstract if article is pay per view) or to the final manuscript accepted for publication (link to article in repository).

<sup>3</sup>

Open Access is defined as free of charge access for anyone via Internet. Please answer "yes" if the open access to the publication is already established and also if the embargo period for open access is not yet over but you intend to establish open access afterwards.

	photon pairs in a poled fiber									
5	Second order nonlinearity in fibers and applications	M. Malmström	American Optics and Photonics Conference, LAOP 2012	10 - 13 November 2012	OSA		2012			no
6	Ytterbium-doped fiber laser mode-locked with electro-optical fiber	M.I Malmström	Europhoton	August 2012	EPS		2012			no
7	Mode-locked fibre laser and amplifier at 1.12µm using ytterbium-doped fibre	L. Lago	Europhoton	August 2012	EPS		2012			no
8	Pulse selection at 1 MHz with electrooptic fiber switch	M. Malmström, O. Tarasenko and W. Margulis	Optics Express		OSA		2012	Opt. Express 20, 9, pp. 9465–9470		yes
9	Loss reduction in periodically poled silica fibres by intense near-UV irradiation	A.V. Gladyshev	ICONO/LAT-2013 conference	Accepted for publication	APS		2013			no
10	Electric field measurement with poled fiber in a Sagnac interferometer	M. Graziosi, W. Margulis, O. Tarasenko	Workshop on Specialty Optical Fibers and their Applications		OSA		2013	paper 3.22		no
11	High-purity, Broadband, Entangled Photon Pairs Generated in Poled Silica Fibers	E. Zhu	Bragg Gratings, Photosensitivity, and Poling in Glass Waveguides (BGPP) 2014	July 2014	OSA		2014	paper: BW1D.1		no
12	Multi-Watt All-Fiber Frequency Doubled Laser (Postdeadline)	C Corbari	Advanced Photonics conference 2014	JTu6A.5	OSA	Barcelona	2014	JTu6A.5	<a href="http://dx.doi.org/10.1364/BGPP.2014.JTu6A.5">http://dx.doi.org/10.1364/BGPP.2014.JTu6A.5</a>	yes

13	All-fiber frequency-doubled visible laser	C. Corbari	Optics Letters	Vol. 39 (22)	OSA		2014	pp. 6505-6508	<a href="http://dx.doi.org/10.1364/OL.39.006505">http://dx.doi.org/10.1364/OL.39.006505</a>	yes
14	Optical fiber poling by induction	F. De Lucia	Optics Letters	Vol. 39 (22)	OSA		2014	pp. 6513-6516	<a href="http://dx.doi.org/10.1364/OL.39.006513">http://dx.doi.org/10.1364/OL.39.006513</a>	yes
14	Specialty fibres and components for advanced microscopy	L. Lago	Specialty Optical Fibers	SoW3B.5	OSA	Barcelona	2014	SoW3B.5	<a href="http://dx.doi.org/10.1364/SOF.2014.SoW3B.5">http://dx.doi.org/10.1364/SOF.2014.SoW3B.5</a>	
15	Study of thermally poled fibers with a two-dimensional model	A Camara	Optics Express	22, 17700-17715	OSA		2014			yes
16	UV-Induced Absorption in All-Fiber Frequency Doublers: Characterization and Photobleaching	A. Gladyshev	Journal of Lightwave Technology	vol.33, Issue 2, January 2015	IEEE		2015	pp. 439 - 442	doi: 10.1109/JLT.2015.2389259	no
17	All-Fiber Polarization-Maintaining Electrooptic Pulse-Picker	M. Malmström, S. Boivinet, O. Tarasenko, J.-B. Lecourt, Y. Hernandez, W. Margulis, and F. Laurell	CLEO US 2015				2015			
18	Optical creation and erasure of the linear electrooptical effect in silica fiber	A. R. Camara, J. M. B. Pereira, O. Tarasenko, W. Margulis and I. C. S. Carvalho	Paper submitted to Opt. Exp				2015			

### 1.6.3.2. List of dissemination activities

TEMPLATE A2: LIST OF DISSEMINATION ACTIVITIES								
NO	Type of activities <sup>4</sup>	Main leader	Title	Date	Place	Type of audience <sup>5</sup>	Size of audience	Countries addressed
1	Conference & exhibition	PQ	17. International Single Molecule Workshop	Sept. 2011	Berlin	Scientific	120	80% Europe, 20% Worldwide
2	Press release	MULT	Visible Improvement	Nov. 2011	Electrooptics Magazine	Scientific		Worldwide
3	Press release	IX	Charming : vers de nouvelles solutions FLIM et STED	Nov. 2011	Revue Photoniques	Scientific		French speaking
4	Exhibition	PQ	Neuroscience	Nov. 2011	Washington D.C.	Scientific	Several 1000s	70% US, 30% worldwide
5	Exhibition	PQ	ASCB	Dec. 2011	Denver	Scientific	Several 1000s	70% US, 30% worldwide
6	Conference & exhibition	PQ	BIOS Single Molecule & High Resolution Imaging	Jan. 2012	San Francisco	Scientific	100 / 7000	Fully international
7	Exhibition	PQ	Photonics West	Jan. 2012	San Francisco	Scientific	More than 10.000	Fully international
8	Conference & exhibition	PQ	Focus on Microscopy	April 2012	Singapore	Scientific	300	Fully international
9	Web	FORC	Charming project. Second order nonlinearity in	22 March 2012	<a href="http://www.fibopt.ru/char">http://www.fibopt.ru/char</a>	Scientific Community		Russian speaking

<sup>4</sup> A drop down list allows choosing the dissemination activity: publications, conferences, workshops, web, press releases, flyers, articles published in the popular press, videos, media briefings, presentations, exhibitions, thesis, interviews, films, TV clips, posters, Other.

<sup>5</sup> A drop down list allows choosing the type of public: Scientific Community (higher education, Research), Industry, Civil Society, Policy makers, Medias ('multiple choices' is possible).

			fibers. From science to applications.		ming.php	(higher education, Research), Industry, Civil Society		
10	Conference & exhibition	MULT	CHARMING	April 2012	Photonics Innovation Village – Photonics Europe - Brussels	Industry, Scientific Community		
11	Press release	FORC	Charming project. Second order nonlinearity in fibers. From science to applications.	April 2012	Journal “Photon-express” #2(98), April 2012	Industry, Scientific Community		Russian speaking
12	Conference	ORC	BGPP 2012, Conference on Bragg Gratings, Photosensitivity and Poling in Glass Waveguides	17-21 June 2012	Colorado Springs	Scientific Community, Industry	~1000	worldwide
13	Conference	IXFIBER ACREO FORC MULT PICOQU ANT	EUROPHOTON	August 2012	Stockholm	Scientific Community, Industry	~200	worldwide
14	Workshop	PICOQU ANT	Workshop on Single Molecule Detection	September 2012	Berlin	Scientific Community,	~100	worldwide
15	Symposium	MULTITE L	17th Annual Symposium of the IEEE Photonics Benelux Chapter colocated with 'Workshop on random fibre lasers'	November 2012	Mons	Scientific Community,, Students	~100	Worldwide
16	Conference	PICOQU	Photonics West 2013	February	San Francisco	Scientific	~1000	worldwide



		ANT		2013		Community,		
17	Conference	PICOQUANT	Focus on Microscopy conference	March 2013	Sydney	Scientific Community,	~1000	worldwide
18	Conference	PICOQUANT	Focus on Microscopy conference	March 2013	Maastrich	Scientific Community,	~1000	worldwide
19	Conference	FORC	ICONO/LAT 2013	June 2013	Moscow, Russia	Scientific Community, Industry	~300	worldwide
20	Conference	FORC	Materials of nano-, micro-, optoelectronics and fiber optics: physical properties and application	October 2013	Saransk, Russia	Scientific Community	~100	Russia
22	Conference	FORC	All-Russian conference on fiber optics	October 2013	Perm, Russia	Scientific Community, Industry	~100	Russia
23	Conference	FORC	The Third China-Russia Bilateral Forum on Materials: Advanced Laser Materials and Laser Techniques	November 2013	Shanghai, China	Scientific Community, Industry	~100	Russia, China
24	Conference	FORC	All-Russian conference on fiber lasers	April 2014	Novosibirsk, Russia	Scientific Community, Industry	~200	Russian speaking
25	Conference	Acreo	Photonics Global Congress (invited paper)	2012	Singapore 2012	Scientific community	~500	Worldwide
26	International workshop	Acreo	“Electric field measurement with poled fiber in a Sagnac interferometer”, Workshop on Specialty Optical Fibers and their Applications WSOF 2013	2013	Sigtuna, Sweden	Scientific community	200	Worldwide
27	Conference	PQ	Pulsed Picosecond 766 nm Laser Source Operating between 1 - 80MHz with Automatic Pump Power Management	February 2013	San Francisco	LASE Scientific	Talk 30 people	USA, world-wide

28	Conference	PQ	Fiber amplified and frequency doubled gain-switched diode laser at 766nm as a depletion source for high resolution STED microscopy	February 2013	San Francisco	BIOS Scientific	Talk 50 people	USA, world-wide
29	Conference	PQ	Freely Triggerable, Diode Based Laser at 766 nm as a Versatile Fluorescence Inhibition Source for STED Nanoscopy and Single Molecule Spectroscopy	March 2013	Maastricht	Microscopy Specialists	Poster	european, world-wide
30	Conference	PQ	New perspectives for ps pulsed laser excitation and multidimensional time-resolved fluorescence analysis	July 2013	Leuven	Life Science specialists	Poster	european, world-wide
31	Conference	PQ	Versatile Pulsed 560 nm Laser Source for Time-resolved Microscopy and Spectroscopy	February 2014, September 2014	San Francisco Berlin	BioPhys	Poster	USA, world-wide, European
32	Conference	PQ	Versatile pulsed 560 nm laser source for FCS and FLCS	February 2014	San Francisco	LASE Scientific	Talk 30 people	USA, world-wide
33	Conference	IXFIBER	ENOVA	September 2014	Paris	Industry, Scientific Community		French speaking
34	Article	PQ	STED Microscopy Made Easy	December 2014	Internet	Scientific	BioPhotonics	world-wide
35	Short Course	ACREO	Optical Fiber Components	Nov 2014	Cancun	Scientific	Invited lecture	world-wide
36	Conference	PQ	Generation of Third Harmonic Picosecond Pulses	February 2015	San Francisco	LASE Scientific	Poster	USA, world-wide

			at 355 nm by Sum Frequency Mixing in Periodically Poled MgSLT Crystal					
37	Conference	PQ	A Freely Triggerable 766 nm Laser with Optimized Performance for STED Applications	February 2015	San Francisco	LASE Scientific	Poster	USA, world-wide
38	Conference	ACREO/ MULTITEL	All-Fiber Polarization-Maintaining Electrooptic Pulse-Picker	May-2015	San Diego	Scientific CLEO US	Oral presentation	USA, world-wide
39	LASER World of PHOTONICS 2015:	MULTITEL	CHARMING - Picosecond fibrelasers in the visible spectrum for biomedical imaging	June 2015	Munich	Scientific Community, Industry	Oral presentation	World-wide

### 1.6.3.3. List of patents and trademarks

PQ was granted the following patent which is part of the main amplifier design needed for higher power levels:

DE 10 2010 037 990.5 (Laservorrichtung)

New patent about hybrid pulse shaping recently filled by PICOQUANT:

DE 2015 001 321.1

## 2. Report on societal implications

### **A General Information** *(completed automatically when Grant Agreement number is entered.*

Grant Agreement Number:

288786

Title of Project:

Components for Highly Advanced time Resolved fluorescence  
Microscopy based on Nonlinear Glass fibres

Name and Title of Coordinator:

Dr Yves Hernandez

### **B Ethics**

#### 1. Did your project undergo an Ethics Review (and/or Screening)?

- If Yes: have you described the progress of compliance with the relevant Ethics Review/Screening Requirements in the frame of the periodic/final project reports?

**NO**

Special Reminder: the progress of compliance with the Ethics Review/Screening Requirements should be described in the Period/Final Project Reports under the Section 3.2.2 'Work Progress and Achievements'

#### 2. Please indicate whether your project involved any of the following issues (tick box) :

**NO**

##### RESEARCH ON HUMANS

- |   |    |
|---|----|
| • Did the project involve children?                         | No |
| • Did the project involve patients?                         | No |
| • Did the project involve persons not able to give consent? | No |
| • Did the project involve adult healthy volunteers?         | No |
| • Did the project involve Human genetic material?           | No |
| • Did the project involve Human biological samples?         | No |
| • Did the project involve Human data collection?            | No |

##### RESEARCH ON HUMAN EMBRYO/FOETUS

- |   |    |
|---|----|
| • Did the project involve Human Embryos?  | No |
| • Did the project involve Human Foetal Tissue / Cells?  | No |
| • Did the project involve Human Embryonic Stem Cells (hESCs)?                                 | No |
| • Did the project on human Embryonic Stem Cells involve cells in culture?                     | No |
| • Did the project on human Embryonic Stem Cells involve the derivation of cells from Embryos? | No |

##### PRIVACY

- |   |    |
|---|----|
| • Did the project involve processing of genetic information or personal data (eg. health, sexual lifestyle, ethnicity, political opinion, religious or philosophical conviction)? | No |
| • Did the project involve tracking the location or observation of people?   | No |

##### RESEARCH ON ANIMALS

- |   |    |
|---|----|
| • Did the project involve research on animals?            | No |
| • Were those animals transgenic small laboratory animals? | No |
| • Were those animals transgenic farm animals?             | No |
| • Were those animals cloned farm animals?                 | No |
| • Were those animals non-human primates?                  | No |

##### RESEARCH INVOLVING DEVELOPING COUNTRIES

- |   |    |
|---|----|
| • Did the project involve the use of local resources (genetic, animal, plant etc)?                        | No |
| • Was the project of benefit to local community (capacity building, access to healthcare, education etc)? | No |

##### DUAL USE

- |                                       |    |
|---------------------------------------|----|
| • Research having direct military use | No |
|---------------------------------------|----|

<ul style="list-style-type: none"> <li>Research having the potential for terrorist abuse</li> </ul>		No
<b>C Workforce Statistics</b>		
<b>3. Workforce statistics for the project: Please indicate in the table below the number of people who worked on the project (on a headcount basis).</b>		
<b>Type of Position</b>	<b>Number of Women</b>	<b>Number of Men</b>
Scientific Coordinator	0	1
Work package leaders	0	5
Experienced researchers (i.e. PhD holders)	2	8
PhD Students	0	0
Other		
<b>4. How many additional researchers (in companies and universities) were recruited specifically for this project?</b>		<b>1</b>
Of which, indicate the number of men:		0

<b>D Gender Aspects</b>		
<b>5. Did you carry out specific Gender Equality Actions under the project?</b>	<input type="radio"/> Yes <input checked="" type="radio"/> X	<input type="radio"/> Yes <input checked="" type="radio"/> No
<b>6. Which of the following actions did you carry out and how effective were they?</b>		
<div style="display: flex; justify-content: space-between;"> <div> <input type="checkbox"/> Design and implement an equal opportunity policy  <input type="checkbox"/> Set targets to achieve a gender balance in the workforce  <input type="checkbox"/> Organise conferences and workshops on gender  <input type="checkbox"/> Actions to improve work-life balance  <input type="radio"/> Other: <span style="border: 1px solid black; display: inline-block; width: 200px; height: 1.2em; vertical-align: middle;"></span> </div> <div style="text-align: center;"> <div style="display: flex; justify-content: space-around; font-weight: bold; font-size: 0.8em;"> <span>Not at all effective</span> <span>Very effective</span> </div> <div style="display: flex; justify-content: space-around;"> <div> <input type="radio"/> <input type="radio"/> <input type="radio"/> <input type="radio"/> <input type="radio"/> </div> <div> <input type="radio"/> <input type="radio"/> <input type="radio"/> <input type="radio"/> <input type="radio"/> </div> </div> </div> </div>		
<b>7. Was there a gender dimension associated with the research content – i.e. wherever people were the focus of the research as, for example, consumers, users, patients or in trials, was the issue of gender considered and addressed?</b> <input type="radio"/> Yes- please specify <span style="border: 1px solid black; display: inline-block; width: 150px; height: 1.2em; vertical-align: middle;"></span> <input checked="" type="radio"/> No		
<b>E Synergies with Science Education</b>		
<b>8. Did your project involve working with students and/or school pupils (e.g. open days, participation in science festivals and events, prizes/competitions or joint projects)?</b> <input type="radio"/> Yes- please specify <span style="border: 1px solid black; display: inline-block; width: 150px; height: 1.2em; vertical-align: middle;"></span> <input checked="" type="radio"/> No		
<b>9. Did the project generate any science education material (e.g. kits, websites, explanatory booklets, DVDs)?</b> <input type="radio"/> Yes- please specify <span style="border: 1px solid black; display: inline-block; width: 150px; height: 1.2em; vertical-align: middle;"></span> <input checked="" type="radio"/> No		
<b>F Interdisciplinarity</b>		
<b>10. Which disciplines (see list below) are involved in your project?</b> <div style="display: flex; justify-content: space-between; align-items: flex-start;"> <div style="width: 45%;"> <input type="radio"/> Main discipline<sup>6</sup>: 2.3  <input type="radio"/> Associated discipline<sup>6</sup>: 3.1         </div> <div style="width: 50%;"> <input type="radio"/> Associated discipline<sup>6</sup>: <span style="border: 1px solid black; display: inline-block; width: 100px; height: 1.2em; vertical-align: middle;"></span> </div> </div>		
<b>G Engaging with Civil society and policy makers</b>		
<b>11a Did your project engage with societal actors beyond the research community? (if 'No', go to Question 14)</b>	<input type="radio"/> Yes <input checked="" type="radio"/> X	<input type="radio"/> Yes <input checked="" type="radio"/> No
<b>11b If yes, did you engage with citizens (citizens' panels / juries) or organised civil society (NGOs, patients' groups etc.)?</b> <input type="radio"/> No <input type="radio"/> Yes- in determining what research should be performed <input type="radio"/> Yes - in implementing the research <input type="radio"/> Yes, in communicating /disseminating / using the results of the project		

<sup>6</sup> Insert number from list below (Frascati Manual).



<b>11c In doing so, did your project involve actors whose role is mainly to organise the dialogue with citizens and organised civil society (e.g. professional mediator; communication company, science museums)?</b>		<input type="radio"/> <input type="radio"/>	Yes No
<b>12. Did you engage with government / public bodies or policy makers (including international organisations)</b>			
<input checked="" type="radio"/> No <input type="radio"/> Yes- in framing the research agenda <input type="radio"/> Yes - in implementing the research agenda <input type="radio"/> Yes, in communicating /disseminating / using the results of the project			
<b>13a Will the project generate outputs (expertise or scientific advice) which could be used by policy makers?</b> <input type="radio"/> Yes – as a <b>primary</b> objective (please indicate areas below- multiple answers possible) <input type="radio"/> Yes – as a <b>secondary</b> objective (please indicate areas below - multiple answer possible) <input checked="" type="radio"/> No			
<b>13b If Yes, in which fields?</b>			
Agriculture Audiovisual and Media Budget Competition Consumers Culture Customs Development Economic and Monetary Affairs Education, Training, Youth Employment and Social Affairs		Energy Enlargement Enterprise Environment External Relations External Trade Fisheries and Maritime Affairs Food Safety Foreign and Security Policy Fraud Humanitarian aid	Human rights Information Society Institutional affairs Internal Market Justice, freedom and security Public Health Regional Policy Research and Innovation Space Taxation Transport

<b>13c If Yes, at which level?</b> <ul style="list-style-type: none"> <li><input type="radio"/> Local / regional levels</li> <li><input type="radio"/> National level</li> <li><input type="radio"/> European level</li> <li><input type="radio"/> International level</li> </ul>		
<b>H Use and dissemination</b>		
<b>14. How many Articles were published/accepted for publication in peer-reviewed journals?</b>		<b>18</b>
<b>To how many of these is open access<sup>7</sup> provided?</b>		<b>8</b>
<b>How many of these are published in open access journals?</b>		<b>8</b>
<b>How many of these are published in open repositories?</b>		<b>0</b>
<b>To how many of these is open access not provided?</b>		<b>10</b>
<b>Please check all applicable reasons for not providing open access:</b>		
<input checked="" type="checkbox"/> publisher's licensing agreement would not permit publishing in a repository <input type="checkbox"/> no suitable repository available <input type="checkbox"/> no suitable open access journal available <input type="checkbox"/> no funds available to publish in an open access journal <input type="checkbox"/> lack of time and resources <input type="checkbox"/> lack of information on open access <input type="checkbox"/> other <sup>8</sup> : .....		
<b>15. How many new patent applications ('priority filings') have been made?</b> <i>("Technologically unique": multiple applications for the same invention in different jurisdictions should be counted as just one application of grant).</i>		<b>1</b>
<b>16. Indicate how many of the following Intellectual Property Rights were applied for (give number in each box).</b>	Trademark	<b>0</b>
	Registered design	<b>0</b>
	Other	<b>0</b>
<b>17. How many spin-off companies were created / are planned as a direct result of the project?</b>		<b>0</b>
<i>Indicate the approximate number of additional jobs in these companies:</i>		
<b>18. Please indicate whether your project has a potential impact on employment, in comparison with the situation before your project:</b>		
<input checked="" type="checkbox"/> Increase in employment, or <input type="checkbox"/> Safeguard employment, or <input type="checkbox"/> Decrease in employment, <input type="checkbox"/> Difficult to estimate / not possible to quantify	<input checked="" type="checkbox"/> In small & medium-sized enterprises <input type="checkbox"/> In large companies <input type="checkbox"/> None of the above / not relevant to the project	
<b>19. For your project partnership please estimate the employment effect resulting directly from your participation in Full Time Equivalent (FTE = one person working fulltime for a year) jobs:</b>		<i>Indicate figure:</i>

<sup>7</sup> Open Access is defined as free of charge access for anyone via Internet.

<sup>8</sup> For instance: classification for security project.

Difficult to estimate / not possible to quantify		X
<b>I Media and Communication to the general public</b>		
<b>20. As part of the project, were any of the beneficiaries professionals in communication or media relations?</b> <input type="radio"/> Yes <input checked="" type="radio"/> No		
<b>21. As part of the project, have any beneficiaries received professional media / communication training / advice to improve communication with the general public?</b> <input type="radio"/> Yes <input checked="" type="radio"/> No		
<b>22 Which of the following have been used to communicate information about your project to the general public, or have resulted from your project?</b>		
<input checked="" type="checkbox"/> Press Release <input type="checkbox"/> Media briefing <input type="checkbox"/> TV coverage / report <input type="checkbox"/> Radio coverage / report <input checked="" type="checkbox"/> Brochures /posters / flyers <input checked="" type="checkbox"/> DVD /Film /Multimedia	<input checked="" type="checkbox"/> Coverage in specialist press <input type="checkbox"/> Coverage in general (non-specialist) press <input type="checkbox"/> Coverage in national press <input type="checkbox"/> Coverage in international press <input checked="" type="checkbox"/> Website for the general public / internet <input type="checkbox"/> Event targeting general public (festival, conference, exhibition, science café)	
<b>23 In which languages are the information products for the general public produced?</b>		
<input checked="" type="checkbox"/> Language of the coordinator <input checked="" type="checkbox"/> Other language(s)	<input checked="" type="checkbox"/> English	